1966

Geometric constraints in electron diffraction analysis; structure of hydrocarbon molecules

Thomas Leslie Boates
Iowa State University

GEOMETRIC CONSTRAINTS IN ELECTRON DIFFRACTION ANALYSIS; STRUCTURE OF HYDROCARBON MOLECULES

by

Thomas Leslie Boates

A Dissertation Submitted to the
Graduate Faculty in Partial Fulfillment of
the Requirements for the Degree of
DOCTOR OF PHILOSOPHY

Major Subject: Physical Chemistry

Approved:

Signature was redacted for privacy.

In Charge of Major Work

Signature was redacted for privacy.

Head of Major Department

Signature was redacted for privacy.

Dean of Graduate College

Iowa State University
of Science and Technology
Ames, Iowa

1966

TABLE OF CONTENTS

INTRODUCTION

Advances in the theory and in experimental techniques of electron scattering by gas molecules have made it possible to determine molecular structures with a precision unattainable a few years ago. Procedures for analyzing diffraction data, however, have not kept pace with developments in theory and experiment. Therefore, the present investigation was initiated (a) to incorporate more complete theoretical expressions into numerical analysis of experimental data, and (b) to carry out analysis directly in terms of internal coordinates of molecules instead of the customary set of (possibility inconsistent) internuclear distances.

An additional objective of the present study was to apply the newly developed methods of analysis to the determination of structures of several molecules. It was hoped that the molecules chosen would serve to illustrate effects of intramolecular Van der Waals forces.

Digital computers have been used extensively to facilitate the extraction of information contained in electron diffraction data. Least squares programs have been developed to solve for a set of internuclear distances giving an optimum fit to the experimental points. In almost all previous analyses the internuclear distances had been allowed to vary independently with no assurance that the final set of distances would correspond to a geometrically possible set. Moreover, when a molecule was studied that contained more internuclear distances than could be varied in a realistic least squares analysis it was necessary to fix the weaker scattering distances at plausible values and allow only the stronger scattering distances to vary. When improved values were found for the major distances

the fixed parameters were recalculated and the process repeated. This process had to be recycled to self-consistency and in many cases it was extremely difficult to obtain a converged set of parameters. It seemed desirable, therefore, to design a computer program which would at all stages treat a molecule in terms of a mutually consistent set of internal structural coordinates. Such an approach would, in general, reduce the number of parameters to be handled and guarantee that the derived internuclear distances would be geometrically compatible. Thus, the tedious recycling required in conventional analysis would be eliminated.

In addition to imposing geometrical constraints, more exact theoretical expressions relating scattered intensities to structural parameters of molecules were incorporated in the least squares programs. Some of the expressions had been too cumbersome to be handled by computers previously available, but have proved to be well within the capabilities of the IBM 7090.

Two least squares programs were developed which imposed geometrical constraints and at the same time incorporated more complete theoretical expressions. The first was for the direct analysis of experimental intensity data and the second was for analysis of the experimental radial distribution curve. Since the radial distribution and intensity functions are related by Fourier transformations, they contain the same molecular information. Nevertheless, in a given situation, one program may have advantages over the other.

These two programs were applied to the structural determinations of hexamethylethane, tetramethylethane and dimethylcyclopropane. All three of the molecules selected are of chemical interest but contain too many

internuclear distances to be handled conveniently by conventional analyzing techniques. A study was also made of the diatomic molecule chlorine to allow a check to be made of the operation of the programs and to provide the investigator with experience in the field of electron diffraction.

The structure of a number of hydrocarbons has been studied in this laboratory. Trends in the structures have been documented and found to be consistent with a simple model of intramolecular Van der Waals forces. The theory of nonbonded interactions predicted deformations from conventional reference configurations when internuclear distances between nonbonded atoms were less than the sums of Van der Waals radii. Hexamethylethane and tetramethylethane are simple hydrocarbons containing methyl groups wedged closely together, but prior to the present study no definite information existed concerning the magnitudes of their steric deformations. The molecule 1,1 dimethylcyclopropane may also be expected to provide information on nonbonded interactions. It may be viewed as a derivative of neopentane in which two of the "methyls" have been tied back by a covalent bond between them (to form the cyclopropane ring). This relieves the stress on the remaining two methyl groups. It is of interest, then, to examine the concomitant relaxation of bonds to these methyl groups.

PREVIOUS WORK

Geometrically Constrained Least Squares Analysis

Reports have been published by two different laboratories indicating that geometric constraints have been employed in the least squares analysis of gas electron diffraction data (1,2). The technique developed by Hedberg *et al* is not conveniently applicable to a complex molecule. It incorporates into the program analytical expressions defining the relationship between the various internuclear distances. These expressions must be developed for each individual type of structure and in a great many molecules such an approach is too tedious to be used. In the method of Corbet *et al*, the independent parameters are chosen to be Cartesian coordinates of atoms. No detailed description of the application of the method has appeared. The procedure does not appear to lend itself readily to the description of a complex molecule and places severe limitations on the choice of the geometrically independent parameters. Very little information has been published on the actual results obtained by applying constraints to the least squares process. The only detailed description in the literature is an application to cyclopropane made by Bastiansen, Fritsch and Hedberg (3).

Molecular Structure Determinations

Many studies have been made of the chlorine molecule. An ultraviolet band spectrum of chlorine was obtained in 1930 by Elliot (4). His results were recalculated by Badger (5) and a complete reinvestigation was made by Richards and Barrow (6). Gas diffraction studies of limited precision were

performed by Richter (7) with X-rays and by Pauling and Brockway with electrons (8). More accurate diffraction studies were performed by Shibata (9) and by Bartell and Carroll (10).

A previous electron diffraction study of hexamethylethane was performed (11). However, the data were not sufficiently developed to establish the exact nature of the steric deformations. A microwave study of the isoelectronic analog $(CH_3)_3B\text{-}N(CH_3)_3$ (12) has been reported by Lide. It was evident that the molecule suffers a considerable deformation but the details of the deformations have been the subject of some controversy. The structures of tetramethylethane and 1,1 dimethylcyclopropane have not been studied. Molecules related to 1,1 dimethylcyclopropane have, however, received considerable attention. An electron diffraction investigation of cyclopropane was conducted by Pauling and Brockway (13). The molecule was reinvestigated recently with greatly improved precision by Bastiansen, Fritsch and Hedberg (3). Cyclopropyl halides have also been investigated. Microwave studies of C_3H_5Cl by Schwendeman, Jacobs and Krigas (14), of $C_3H_4Cl_2$ by Flygare, Narath and Gwinn (15) and of C_3H_5Cl by Friend and Dailey (16) have been published.

THEORETICAL EXPRESSIONS USED IN GAS ELECTRON DIFFRACTION

Theoretical expressions for the scattering of high energy electrons by molecules were developed by Mott (17), Wierl (18) and Debye (19). Corrections for anharmonicity of vibration (20), failure of the Born Approximation (21,22,23) and finite beam energy (24) have been added to the original expressions in recent years.

When high energy electrons encounter a molecule they are scattered by both the planetary electrons and the atomic nuclei. If the energy of the incident electrons is large compared to the energy of the bound planetary electrons, the intensity scattered by an N atom molecule is given by

$$I_{total}(s) = \frac{K}{R^2 s^4} \{ \sum_{i=1}^{N} [(Z_i - F_i(s))^2 + S_i(s)] + \sum_{i}^{N} \sum_{j \neq i}^{N} (Z_i - F_i(s))(Z_j - F_j(s)) \int_0^{\infty} (P_{ij}(r) \sin sr/sr) dr \} \quad (1)$$

$$= I_{atomic} + I_{molecular}$$

where s is the scattering variable, $F_i(s)$ and $S_i(s)$ are the elastic and inelastic X-ray scattering factors, respectively, for the i^{th} atom, $P_{ij}(r)$ the probability distribution function for the separation of the i^{th} and j^{th} atom, R the distance from the point of interaction to the point of observation and K is related to the incident electron beam intensity and the number of atoms encountering the beam (25). The scattering variable is given by

$$s = \frac{4\pi}{\lambda} \sin \frac{\theta}{2} \quad (2)$$

where λ is the wavelength of the incident electron beam and θ is the scattering angle.

It is convenient in structural analysis to work with a reduced intensity function M(s), where

$$M(s) = \frac{I_{molecular}}{I_{atomic}} = [\frac{I_{total}}{I_{atomic}} - 1] \quad . \tag{3}$$

If the $P_{ij}(r)$ are approximated by Morse distribution functions (26) and corrections for failure of Born approximation included, the theoretical reduced intensity function may be expressed as

$$M(s)_{theor} = \sum_i \sum_{j \neq i} C_{ij} U_{ij}(s) \exp[(-\ell_m^2)_{ij} s^2/2](\cos\Delta\eta_{ij})$$

$$X \sin [s((r_a)_{ij} + \phi_{ij}(s))]/s(r_e)_{ij} \tag{4}$$

where $C_{ij} = Z_i Z_j / \sum_{k=1}^{N} (Z_k^2 + Z_k)$

$$U_{ij}(s) = [Z_i - F_i(s)][Z_j - F_j(s)]$$

$$/ [C_{ij}(Z_k - F_k(s))^2 + S_k(s)]$$

$(\ell_m)_{ij}$ is the effective root mean square amplitude of vibration of the ij^{th} atom pair (27),

$\cos\Delta\eta_{ij}$ is the phase shift correction for failure of Born Approximation (21,22,23) for ij^{th} distance,

$(r_a)_{ij}$ is the center of gravity of the ij^{th} distribution $P_{ij}(r)/r$ (27),

$\phi_{ij}(s)$ is the frequency modulation term associated with the ij^{th} anharmonic oscillator (27), and

$(r_e)_{ij}$ is the equilibrium distance for the ij^{th} atom pair.

EXPERIMENTAL PROCEDURE

Apparatus

The electron diffraction unit used in this investigation was constructed at Iowa State University. It is similar to the apparatus constructed at the University of Michigan by Brockway and Bartell (28).

The electron beam was accelerated through a 40,000 volt potential difference and focussed with a magnetic lens to a spot 0.05 millimeter in diameter on the photographic plate. The diffraction patterns were recorded on Kodak 4" x 5" process plates. A heart-shaped sector was rotated above the plates to compensate for the steep dropoff in intensity of the scattered electrons with increasing scattering angle.

The gas sample was introduced at right angles to the electron beam through a platinum nozzle which could be placed 21 centimeters, 11 centimeters or 7 centimeters above the photographic plate. This allowed data to be recorded from $s \approx 3.5 \text{Å}^{-1}$ to $s \approx 65 \text{Å}^{-1}$. The distance between the platinum nozzle and photographic plate was measured with a high-precision cathetometer.

The specimen injection system consisted of the platinum nozzle, a sample bulb and a stopcock-microswitch attachment. Whenever the stopcock was opened, the microswitch triggered an electrostatic shutter so that the electron beam and the emerging gas sample intersected for a specified length of time. The sample pressure and exposure time were controlled to reduce pressure buildup in the diffraction chamber. A liquid nitrogen trap was also placed in the diffraction chamber to condense the gas sample after it had intersected the electron beam.

Intensities of diffraction patterns were determined by measuring the absorbancies of four plates for each camera distance. The measurements were made with a modified Sinclair-Smith microphotometer in conjunction with a voltage-to-frequency converter and a Hewlett-Packard electronic counter-digital recorder assembly. During photometry the plates were rotated so that three complete revolutions occurred in the one-second reading period to average over the grains in the photographic emulsions. Voltage readings were recorded at quarter-millimeter intervals starting at the outer edge to the right of pattern center and progressing across the center to the opposite edge. Since readings were made both to the right and to the left of the pattern center, eight measurements in all were averaged at each particular value of s. Furthermore, reading the full diameter of the diffraction pattern eliminated small errors in centering the spinning plate.

The exposure time, camera distances and other parameters defining the experimental conditions under which the diffraction patterns of the various molecules were obtained are indicated in Table 1.

Experimental Intensity Curve

After the photographic plates were read with the microphotometer, the mean absorbancies $\overline{A}$ were calculated

$$\overline{A} = (A_R + A_L)/2$$

where the subscripts R and L refer to data taken to the right and left of center, respectively, and

$$A_R = \log[(V_{100} - V_0)/(V_R - V_0)]$$

Table 1. Experimental conditions under which diffraction patterns were obtained

Molecule	Camera Distance (mm)	Exposure Time (sec)	Sample Temperature (°C)	Sample Pressure (mm Hg)	Beam Current (μa)	Emulsion Calibration Constants α_1, α_2
chlorine	210.48	1.4	25	24	0.504	0.50, 0.00
	111.07	3.5	25	30	0.686	0.50, 0.00
hexamethylethane	213.62	6.0	32	32	0.616	0.50, 0.00
Run I	110.83	16.0	23	22	0.616	0.50, 0.00
	67.74	30.0	28	29	0.616	0.50, 0.00
hexamethylethane	214.35	5.0	25	24	0.490	-0.28, 0.14
Run II	106.32	16.0	25	24	0.490	-0.28, 0.14
	68.15	24.0	25	24	0.532	-0.28, 0.14
tetramethylethane	214.35	12.0	-35	10	0.490	-0.28, 0.14
	106.32	10.0	- 7	55	0.497	-0.28, 0.14
	68.15	16.0	- 7	55	0.525	-0.28, 0.14
1,1 dimethyl-	213.61	7.4	25	25	0.392	-0.28, 0.14
cyclopropane	106.72	10.0	25	60	0.399	-0.28, 0.14
	67.70	25.5	25	60	0.406	-0.28, 0.14

$$A_L = \log[(V_{100} - V_0)/(V_L - V_0)]$$

$$V_0 = V_0^i + Y'(r)\ (V_0^f - V_0^i)$$

$$V_{100} = V_{100}^i + Y'(r)(V_{100}^f - V_{100}^i)$$

where $Y'(r)$ is a measure of the instrumental drift and is equal to $Y_R(r)$

$$Y_R(r) = [r_{max} - r]/\ [2(r_{max} - r_{min})]$$

when the readings are to the right of center. $Y'(r)$ is equal to $Y_L(r)$

$$Y_L(r) = 1 - Y_R(r)$$

when the readings are to the left of center.

The parameter r is the distance from the center of the pattern and varies between r_{min} and r_{max}, V_0^i and V_0^f are the initial and final dark current readings, and V_{100}^i and V_{100}^f are the initial and final voltage readings at an unexposed portion of the photographic plate.

A plot of the difference between the readings to the right and those to the left of center indicates the centering error for the particular plate and the amount of random scatter in the readings caused by the microphotometer fluctuations. A set of absorbancies was considered usable if the undulation due to the centering error was less than 0.5 percent and the random fluctuations less than 0.1 percent of the absorbancies.

The average absorbancies were converted to average intensities by

$$\bar{I} = \sum_{i=1}^{M} \bar{A}_i (1 + \sum_{n=1}^{2} \alpha_n A^n)/M$$

where α_n's are the emulsion calibration constants (29) and M is the number

of plates to be averaged. The average intensities are then leveled by the expression

$$I_0(s) = (\bar{I} - I_e)(1 + (r/L)^2)^3(\phi_{sc}/r^3)/I_{atomic}$$

where the quantity $(1 + (r/L)^2)^3$ corrects for the inverse square falloff of the intensity received by the flat photographic plate. The sector correction term is (ϕ_{sc}/r^3) and the extraneous scattering I_e is obtained by reading a plate which was exposed to the electron beam without introducing the gas sample into the diffraction chamber. The theoretical expression for the atomic scattering, I_{atomic}, used to level the intensities is given by

$$I_{atomic} = \sum_{k=1}^{N} [(Z_k - F_k(s))^2 + S_k(s)] .$$

Analytical functions approximating $F_k(s)$ and $S_k(s)$ were used to calculate the elastic and inelastic scattering factors at arbitrary s values. A function of the form

$$F_k(s) = \sum_j a_j/(1 + b_j s^2)^{\ell_j}$$

was used to approximate the elastic scattering factor (30,31). The Heisenberg-Bewilogua (32,33) approximation was used to calculate $S_k(s)$ values.

Experimental reduced intensity data, $M(s)_{exp}$, were obtained from the leveled intensity by dividing $I_0(s)$ by an experimental background function $I_B(s)$. If theory and experiment were perfect, $I_B(s)$ would be constant for all s values. Since, however, the theoretical expressions for atomic scattering are only approximations, and extraneous scattering cannot be determined accurately, the background is not constant and a smooth curve must be

selected to represent $I_B(s)$. The leveled intensity curve is divided by the smooth curve $I_B(s)$ to obtain $M(s)_{exp}$

$$M(s)_{exp} = [I_0(s)/I_B(s) - 1] .$$

Experimental Radial Distribution Curve

The radial distribution function is often defined (34) as

$$f(r) = \int_0^\infty sM(s) \exp(-bs^2) \sin sr \, ds$$

where $\exp(-bs^2)$ is the Degard damping factor (35). As can be seen from Equation 4, the reduced intensity includes effects of planetary electron scattering in the term $U_{ij}(s)$. It is convenient in structural studies to make some correction for this non-nuclear scattering before inversion of the data to facilitate the deduction of internuclear distances. Plotted in Figure 1 are $U_{ij}(s)$ functions computed for the three different types of bonds in hexamethylethane. The limit of $U_{ij}(s)$ as s approaches infinity is unity, but the deviation from unity is appreciable at small values of s. Several different methods have been proposed to compensate for the contribution of the planetary electrons (34,35,36,37) to the molecular intensity. The approach used in this study was to approximate the $U_{ij}(s)$ functions with Gaussian functions of the form

$$N_{ij}(s) = a_{ij} + b_{ij}\exp(-\beta_{ij}s^2)$$

where a_{ij}, b_{ij} and β_{ij} are constants. A comparison of $N_{ij}(s)$ and $U_{ij}(s)$ is shown in Figure 1. A corrected reduced intensity function $M_N(s)$ was defined as

Figure 1. A comparison of U_{ij} and N_{ij} curves for three bond types in hexamethylethane

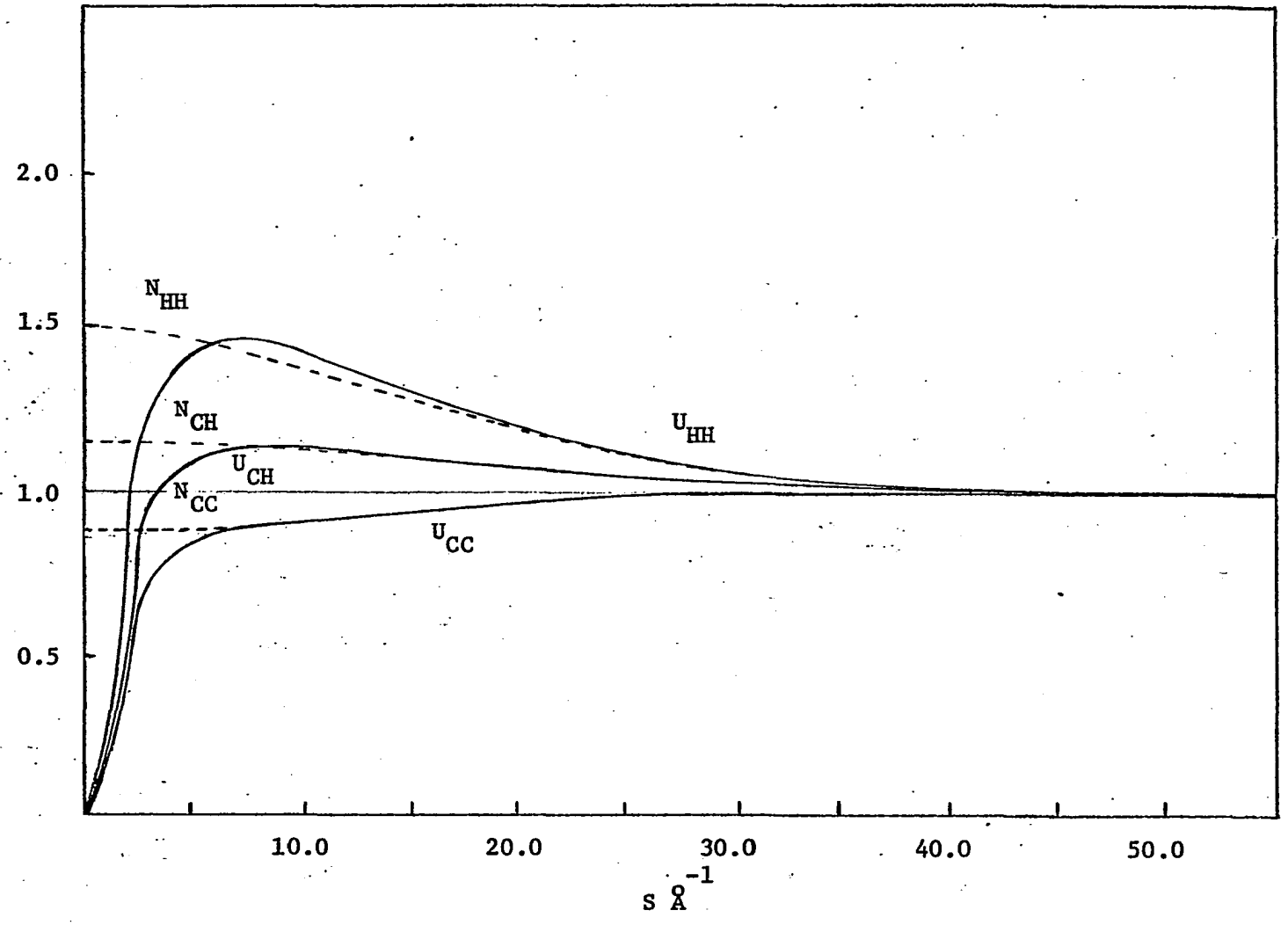
2.0
1.5
1.0
0.5
N_{HH}
N_{CH}
N_{CC}
U_{HH}
U_{CH}
U_{CC}
10.0
20.0
30.0
40.0
50.0
s Å^{-1}

$$M_N(s) = \sum_i \sum_{j\neq i} C_{ij} N_{ij}(s) \exp[(-\ell_m^2)_{ij} s^2/2](\cos\Delta\eta_{ij})$$

$$X \sin[s(r_a)_{ij} + \phi_{ij}(s)]/s(r_e)_{ij}$$

and the related distribution curve as

$$f_N(r) = \int_0^\infty sM_N(s) \exp(-bs^2) \sin sr \, ds. \qquad (6)$$

The procedure employed was to convert $M(s)_{exp}$ to $M_N(s)_{exp}$ by use of a calculated function $\Delta M(s)$ where

$$\Delta M(s) = \sum_i \sum_{j\neq i} C_{ij}(U_{ij} - N_{ij}) \exp[(-\ell_m^2)_{ij} s^2/2](\cos\Delta\eta_{ij})$$

$$X \sin[s(r_a)_{ij} + \phi_{ij}(s)]/s(r_e)_{ij}. \qquad (7)$$

The corrected experimental reduced intensity

$$M_N(s)_{exp} = M(s)_{exp} + \Delta M(s)$$

was then used to obtain $f_N(r)_{exp}$.

Since experimental data are not available for very small and very large values of s, theoretical $M_N(s)$ data were used in the region $s = 0$ to $s = s_{min}$ and an integral termination correction, I_{term}, (36) was applied to make allowance for lack of data from $s = s_{max}$ to $s = \infty$.

Experimental radial distribution curves were calculated from

$$f_N(r)_{exp} = \sum_{s=0}^{s_{min}} sM_N(s)_{theo} \exp(-bs^2)(\sin sr)\Delta s$$

$$+ \sum_{s=s_{min}}^{s_{max}} sM_N(s)_{exp} \exp(-bs^2)(\sin sr)\Delta s + I_{term}. \qquad (8)$$

GEOMETRICALLY CONSTRAINED LEAST SQUARES ANALYSIS

Application of Constraints

The $N(N - 1)/2$ internuclear distances found in an N atom molecule are not, in general, all independent but may be expressed as functions of $3N - 6$ geometrically independent parameters ($N > 2$). Geometrical constraints may be imposed on the $N(N - 1)/2$ internuclear distances by relating the positions of the atoms in the molecule to the $3N - 6$ independent parameters which define the geometry.

Geometrical constraints are imposed in the present analysis by choosing coordinate systems for each of the atoms in the molecule so that atom A_i is located at the origin of its coordinate system with the x_i axis lying along the bond joining atom A_i and atom A_{i-1} and the y_i axis in the plane defined by atoms A_{i-1}, A_i and A_{i+1}. For atom A_1 the x_1 and y_1 axes are arbitrarily set in some convenient direction. With the use of these coordinate systems it is easy to write the coordinates of atom A_i in the A_{i-1} coordinate system and then to transfer stepwise back to the coordinate system for atom A_1. A matrix method due to Eyring (40) can be used in the transformation. The matrix elements are functions of R_i, a displacement along the x_i axis; α_i, a rotation about the z_i axis such that the x_i axis is coincident with x_{i-1} axis, and β_i a rotation about the displaced y_i' axis so that the z_i axis is coincident with z_{i-1} axis. This allows a set of internal coordinates to be chosen as the independent parameters that are varied in the least squares calculations. With a little practice and judicious use of dummy atoms, it is possible to formulate descriptions of quite complex molecules with this approach and to impose whatever symmetry restrictions

are desired. The R_i's, α_i's and β_i's are expressed as linear functions of the chosen set of independent parameters. This permits the most convenient set of internal coordinates to be chosen as the independent parameters. For example, the set may be composed of bond lengths, average bond lengths, a difference in bond lengths, bond angles, a difference in bond angles, average bond angles, and internal rotations about a given bond. Once the coordinates of all atoms are determined, the internuclear distances are calculated using the following equation:

$$r_{ij} = [(x_i - x_j)^2 + (y_i - y_j)^2 + (z_i - z_j)^2]^{\frac{1}{2}}. \qquad (9)$$

To demonstrate the application of geometrical constraints to the least squares analysis of data it is convenient to begin by summarizing the principles of least squares curve fitting. Following formulation of Hedberg (1) we suppose

$$f = f(x_1, x_2, x_3 \ldots\ldots x_m)$$

is a nonlinear function of m parameters x_q by which we seek to represent K (K > m) experimental points. If approximate values x^0 are known for the m parameters, we have, neglecting higher order terms,

$$f = f(x_1^0, x_2^0, x_3^0 \ldots\ldots x_m^0) + (\delta f/\delta x_1)_0 \Delta x_1$$

$$+ (\delta f/\delta x_2)_0 \Delta x_2 + \ldots\ldots\ldots\ldots$$

or in matrix notation

$$F_K = F_K^0 + A_{Km} X_m . \qquad (10)$$

Equations 10 are the conditional equations. F_K and F_K^{obs} differ by V_K, so that use of the observed values of the function gives, after dropping subscripts,

$$F^{obs} + V = F^0 + AX$$

$$V = F^0 - F^{obs} + AX = -N + AX. \tag{11}$$

Introducing the diagonal weight matrix $P_{KK} = P$ and applying the least squares criterion $V'PV \rightarrow$ minimum (V' is the transpose of V) we have

$$(\delta/\delta X)\ (V'PV) = A'PV = 0. \tag{12}$$

Combination of Equations 11 and 12 gives the normal equations

$$BX = Y$$

where

$$B = A'PA$$

and

$$Y = A'PN.$$

The solutions are

$$X = B^{-1}Y, \tag{13}$$

and the standard errors $\sigma(x_q)$ are

$$\sigma(x_q) = [(B^{-1}_{qq})(V'PV)/(K - m)]^{\frac{1}{2}}. \tag{14}$$

Elements in the matrices are of the following form

$$y_q = \sum_{n=1}^{K} (\delta f_n/\delta x_q)_o (f_n - f_n^{obs})\ w_n$$

$$b_{qk} = \sum_{n=1}^{K} (\delta f_n/\delta x_q)_o (\delta f_n/\delta x_k)_o w_n$$

where n ranges over the points in the experimental curve and w_n is the weight function. To obtain improved values for the geometrically independent parameters, the partial derivatives in the matrices B and Y must represent the change in the function with respect to the geometrically independent parameters z_k such that

$$b_{qk} = \sum_{n=1}^{K} (\delta f_n/\delta z_q)_o (\delta f_n/\delta z_k)_o w_n .$$

Since expressions for the experimental curves in electron diffraction are in terms of the internuclear distances and amplitudes of vibration, the required partial derivatives are obtained by

$$(\delta f_n/\delta z_k)_o = \sum_i \sum_{j \neq i} (\delta f_n/\delta r_{ij})_o (\delta r_{ij}/\delta z_k)_o .$$

A numerical value of $(\delta r_{ij}/\delta z_k)_o$ is obtained by calculating a set of r_{ij} from the independent parameters $z_1, z_2 \ldots z_k \ldots z_m$ and a second set r'_{ij} from the independent parameters $z_1, z_2, \ldots\ldots z_k + \Delta z_k \ldots\ldots z_m$. If Δz_k is small, then

$$(\delta r_{ij}/\delta z_k)_o \simeq [(r'_{ij} - r_{ij})/\Delta z_k]_o .$$

This allows corrections to be obtained for the independent parameters. The improved values may then be used to recalculate values for internuclear distances and partial derivatives. The process can be repeated until a converged set of independent parameters is obtained.

The geometrically consistent parameters calculated by Equation 9 are not, however, equivalent to the observed mean internuclear distance r_g.

The geometrically consistent parameters are calculated for a rigid molecule. Since the atoms are in a constant state of vibration, the observed lengths of nonbonded distances are different from the geometrically

consistent nonbonded distances. This effect is known as the Bastiansen-Morino shrinkage effect (41,42,43). Estimated values of the shrinkage effects are subtracted from distances calculated by Equation 9 and the corrected values used in the least squares calculations.

In practice it is not feasible to vary all the amplitudes of vibration associated with the $N(N - 1)/2$ internuclear distances in a least squares analysis. The number of amplitudes allowed to vary should not exceed the number of distinguishable peaks in the radial distribution curve. Therefore, provision is made in the least squares programs allowing two or more of the $N(N - 1)/2$ distances to be defined as either having identical amplitudes of vibration or amplitudes that differ by a fixed amount. If there are two bonds in the molecule which are slightly different in length but are otherwise similar, it is possible to use an extension (44) of Badger's rule (5) to estimate the difference in the two amplitudes. According to Badger's rule the force constant k is related to the internuclear distance r_{ij} by

$$k(r_{ij} - d_{ij})^3 = 1.86 \times 10^5$$

where d_{ij} is a constant tabulated by Badger and is dependent on the two elements comprising the bond. If the amplitude of vibration can be considered to be inversely proportional to the fourth root of the force constant, as in the case of a diatomic molecule, then the amplitude ℓ_2 of bond r_2 can be related to the amplitude ℓ_1 of bond r_1 by

$$\ell_2/\ell_1 = [(r_1 - d_{ij})/(r_2 - d_{ij})]^{3/4}. \qquad (15)$$

Least Squares Intensity Analysis

The calculations performed by the geometrically constrained least squares analysis of the intensity curve are similar to those described in Reference 45 except for the imposition of geometrical constraints. The criterion for refinement is minimization of the weighted sum over experimental points

$$\sum_i w_i [(I_o(s))_{calc} - (I_o(s))_{obs}]_i^2$$

with respect to variation of both molecular parameters and experimental background. The calculated intensity is given by

$$I_o(s)_{calc} = I_B(s)[1 + RM(s)_{theo}]$$

where R is the index of resolution, $I_B(s)$ is an analytical function of the form

$$I_B(s) = a_o \exp(-\delta s) + \sum_{n=1}^{N} a_n s^{n-1} \qquad (16)$$

and $M(s)_{theo}$ is defined by Equation 4. The experimental background was varied in the least squares analysis by allowing the background coefficients a_n to change in the least squares iterations.

The intensity data were weighted by a simple function of s to account for the uncertainty in the loose ends of $I_B(s)$ and to weight down the data at small scattering angles where the imperfections in the sector figure are known less reliably. The weighting function chosen in this investigation is of the form

$$w_i(s) = \exp[-\rho(s - s_B)^2][b - \exp(-\sigma(s - s_A)^2)] \qquad (17)$$

where ρ, s_B, b, σ and s_A are constants.

Least Squares Radial Distribution Analysis

The least squares technique developed by Bonham and Bartell (37) that has previously been used in analysis of radial distribution curves was developed to fit the observed peaks in the curves with Gaussian functions. This required that initial guesses of molecular parameters be used in construction of the distribution curve in order to

(a) correct for the anharmonic character of the peaks

(b) fill in data from s = 0 to s_{min}

(c) correct the reduced intensity function $M(s)_{exp}$ to a constant coefficient function $M_c(s)_{exp}$.

The constant coefficient function $M_c(s)$ has the same form as the $M_N(s)$ function defined by Equation 5 if the term N_{ij} is taken to be unity.

Although this procedure did not prejudice the experimental result to any great extent if it were recycled to self-consistency, it was clumsy and tedious to use. The constrained least squares program was designed to fit an $f_N(r)_{exp}$, obtained from $M_N(s)_{exp}$, with an anharmonic radial distribution function. The influence of the initial structural guesses is, therefore, reduced since

(a) the $M_N(s)$ curve more closely approximates the M(s) curve than does the $M_c(s)$ curve

(b) no corrections for the anharmonic character of the distribution peaks are made in the construction of the experimental curve.

A theoretical curve is still used to fill in the region from s = 0 to s_{min} in the construction of the distribution curve. Experience has shown that

minor inconsistencies in calculating the theoretical $M_N(s)$ in this range have little effect on the position of narrow peaks in $f_N(r)$ curves. Peaks occurring at large r with large amplitudes of vibration, however, may be quite sensitive to the input curve and hence should not be relied upon to determine the structural parameters.

The criterion for refinement in the least squares analysis of the $f_N(r)$ curve is minimization of the sum over all points in the radial distribution curve

$$\sum_i [f_N(r)_{exp} - f_N(r)_{calc}]_i^2$$

with respect to variation of a set of geometrically independent parameters and amplitudes of vibration. It can be shown that the radial distribution function $f_N(r)$ is related to the probability distribution by (27)

$$f_N(r) = \sum_i \sum_{j \neq i} A_{ij} c_{ij} \{a_{ij} [\pi/16b]^{\frac{1}{2}} \int_{-\infty}^{\infty} P_{ij}(x) (r_e + x)_{ij}^{-1}$$

$$X \exp[-(r - r_e - x)^2/4b] \, dx + c_{ij} b_{ij} [\pi/16(b + \beta_{ij})]^{\frac{1}{2}} \int_{-\infty}^{\infty} P_{ij}(x)$$

$$X (r_e + x)_{ij}^{-1} \exp[-(r - r_e - x)^2/4(b + \beta_{ij})] \, dx\}$$

If the Morse oscillator distribution function (26) is used to represent $P_{ij}(r)$, then

$$f_N(r)_{calc} = \sum_i \sum_{j \neq i} A_{ij} [c_{ij}/(2(r_e)_{ij})] \{a_{ij} [(\alpha_{ij}/\gamma_{ij})^{\frac{1}{2}} E(x)_{ij}$$

$$\exp(-\alpha_{ij} x_{ij}^2/\gamma_{ij}) + b_{ij} [(\alpha_{ij}/\gamma'_{ij})^{\frac{1}{2}} E'(x)_{ij}$$

$$\exp(-\alpha_{ij} x_{ij}^2/\gamma'_{ij})]\}, \qquad (18)$$

where

$$E(x)_{ij} = \sum_{n=0}^{5} (\varepsilon'_n)_{ij} \gamma_{ij}^{-n} x^n_{ij}$$

$$E'(x)_{ij} = \sum_{n=0}^{5} (\varepsilon'_n)_{ij} \gamma'^{-n}_{ij} x^n_{ij}$$

$$\gamma_{ij} = 4b\alpha_{ij} + 1$$

$$\gamma'_{ij} = 4(b + \beta_{ij})\alpha_{ij} + 1$$

$$(\varepsilon'_n)_{ij} = \sum_{m=0} (n + 2m)!/(2^m n!m!)(d_{n+2m})_{ij} g^m_{ij} \quad (n,m=0,1,2,3,\ldots.)$$

$$g_{ij} = 1/2\alpha_{ij} \qquad \alpha_{ij} = 1/2(\ell_\alpha)^2_{ij}$$

$$(d_n)_{ij} = (c_n)_{ij} - (d_{n-1})_{ij}/(r_e)_{ij} \qquad \text{with } d_0 = 1$$

$$x_{ij} = r - (r_e)_{ij} ,$$

and A_{ij} is a normalizing constant, b the constant term in the Degard damping factor; a_{ij}, b_{ij} and β_{ij} are the constants defining the N_{ij} curves, and $(c_n)_{ij}$ are a set of parameters which are functions of $(\ell_\alpha)_{ij}$ and a_{ij} the Morse asymmetry constant. The $(r_e)_{ij}$, $(\ell_\alpha)_{ij}$ and a_{ij} are convenient parameters for expressing the radial distribution function. The more physically significant parameters r_g and ℓ_g are derived from these parameters by use of Equations 8 and 19 in Reference 27. It has been found that the first five terms in the sum $E(x)_{ij}$ characterize the anharmonic character of the distribution curve with sufficient accuracy for current needs.

If corrections are needed for the failure of the Born approximation, the first three terms in the series $E(x)_{ij}$ and $E'(x)_{ij}$ are replaced by an expression developed by Bonham and Ukaji (21). When the difference in atomic number is very large, the expression of Bonham and Ukaji breaks down and

some additional terms are needed. These terms were developed by Kimura and Iijima (46). The values of the integrals of Kimura and Iijima are determined in the program, numerically, using Gauss's quadrature method. A synthetic radial distribution curve was obtained from a theoretical $M_N(s)$ curve for a hypothetical model of XeF_2 to check the validity of the expressions in the least squares program. A comparison is made in the Appendix of the two distribution curves, one developed from the inverse of $M_N(s)$, the other from expressions in the constrained least squares program.

ANALYSIS OF DATA

Chlorine

Leveled experimental intensities and experimental backgrounds for 21-centimeter and 11-centimeter camera distances are shown in Figure 2. The backgrounds were adjusted to eliminate negative regions in the radial distribution curve. A radial distribution curve was constructed using a damping factor $\exp(-.00168s^2)$. The radial distribution curve is shown in Figure 3.

Results of the least squares analyses of the intensity curves, an anharmonic radial distribution curve and an analysis of a "harmonic" distribution curve analyzed using the least squares method of Bonham and Bartell are indicated in Table 2. The standard deviation of the parameters $\sigma(x_q)$, calculated by the least squares programs are included in the table along with estimates of the total standard deviations, including random and systematic errors.

The spectroscopic results of Richards and Barrow (6) are also reported in the table. Values of ℓ_α and r_g were calculated from the reported values r_e, ν_e and a_{ij} in order to compare these results with electron diffraction results. A value for ℓ_α was calculated from ν_e by use of Equation 2 in Reference 27. The value of r_g was obtained from r_e, a_{ij} and ℓ_α by use of Equation 12 in Reference 27. Since the electron diffraction patterns were obtained at 25°C an additional 0.001Å was added to the value of r_g calculated using Equation 12. This value approximates the amount of centrifugal stretch experienced by the chlorine molecule at 25°C (20).

Figure 2. Chlorine intensity and experimental background curves for long and middle camera distances

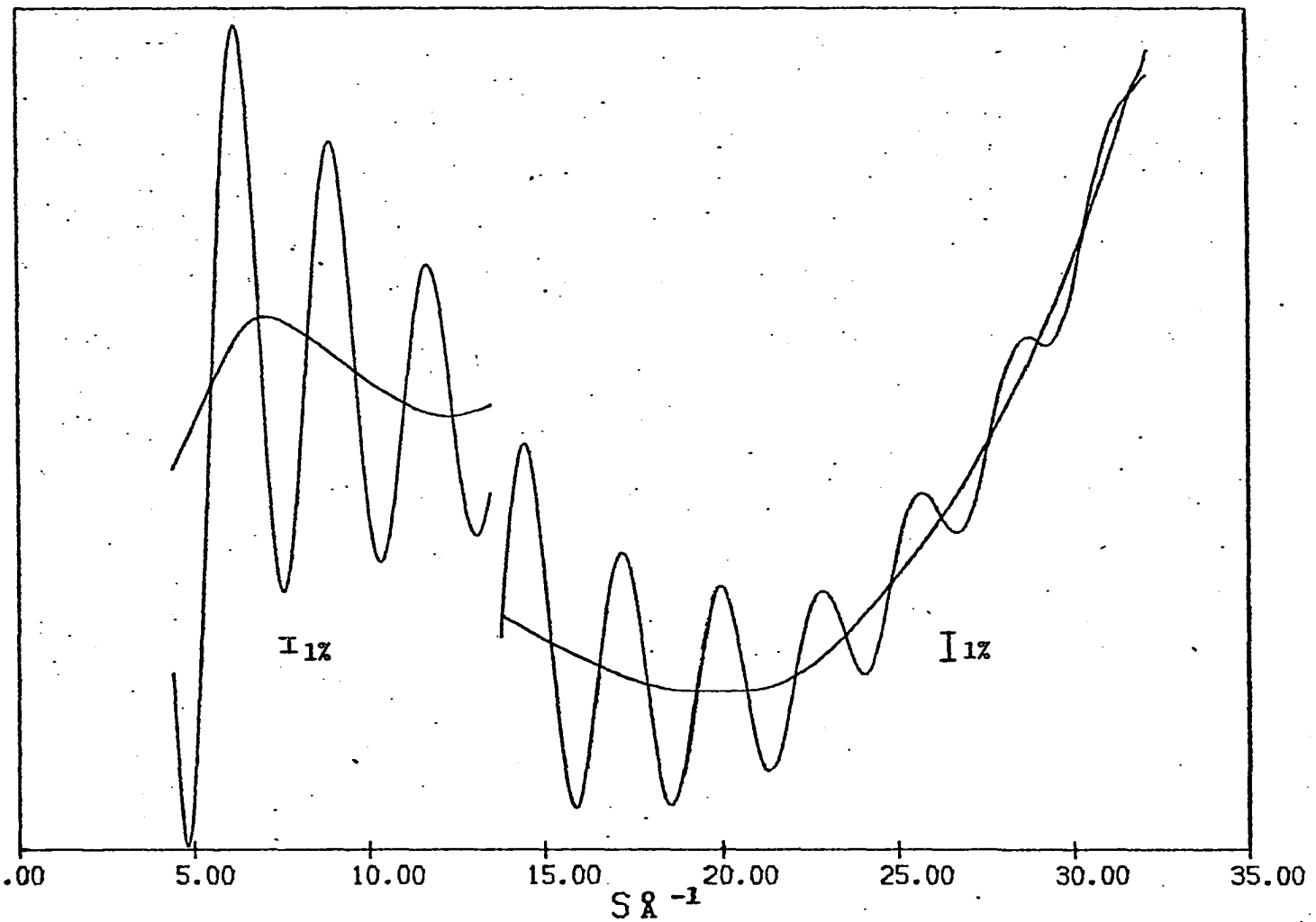
I 1%
I 1%
.00
5.00
10.00
15.00
20.00
25.00
30.00
35.00
S Å -1

Figure 3. Anharmonic radial distribution curve of chlorine. Constructed with N_{ClCl} equal to unity. Theoretical curve shown with crosses.

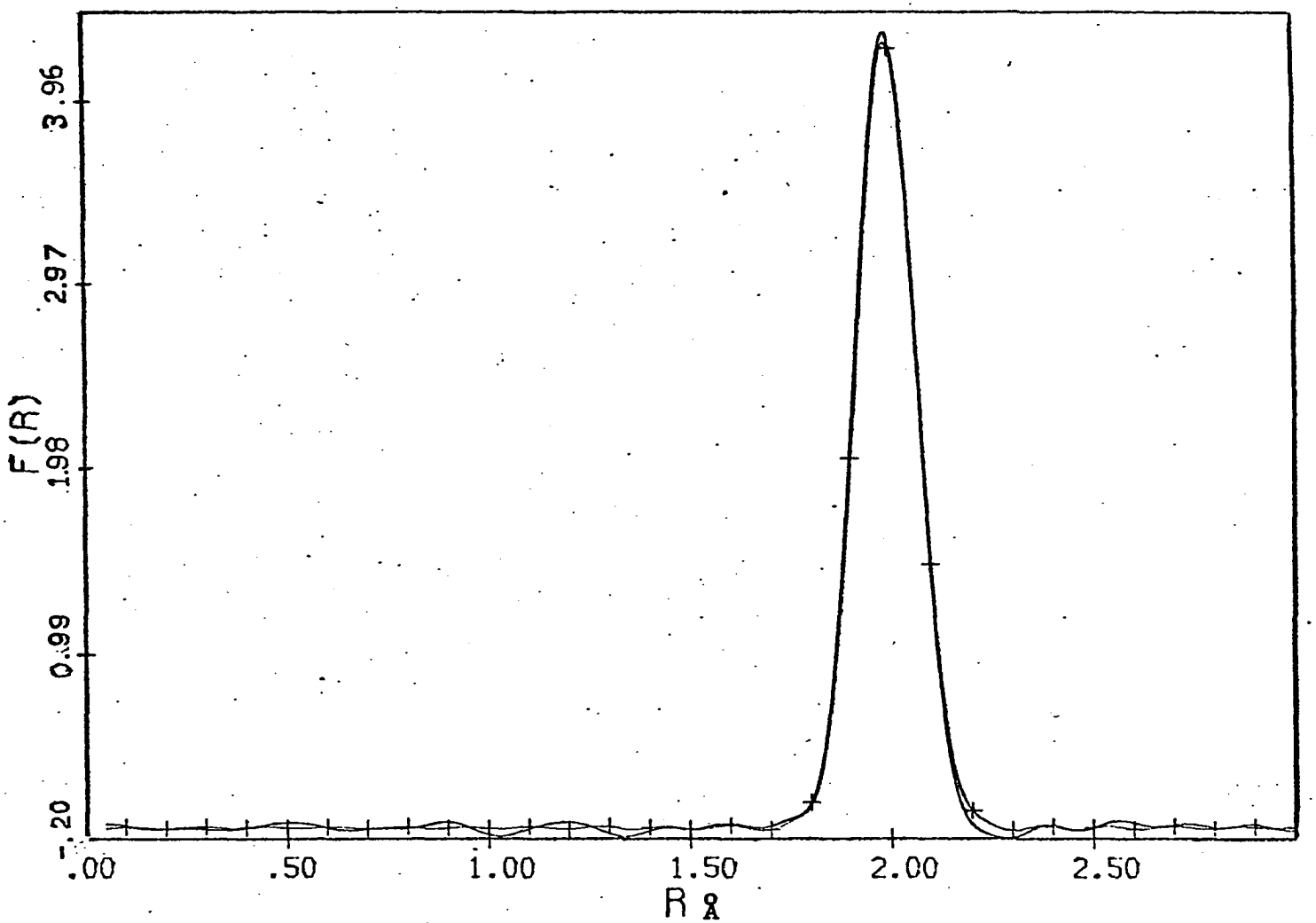
F(R)
3.96
2.97
1.98
0.99
-.20
.00
.50
1.00
1.50
2.00
2.50
R Å

Table 2. Results of chlorine studies

Studied by	r_g	$\sigma(r_g)$	$\ell\alpha$	$\sigma(\ell\alpha)$
Carroll and Bartell	$1.992_7 \pm 0.0045$[a]		$0.043_9 \pm 0.0021$[a]	
Shibata	$1.994_0 \pm 0.0025$		0.050 ± 0.003	
Richards and Barrows	1.994_4		0.041_5	
Least Squares Analyses				
of Long $I_o(s)$	1.991_9	0.00037	0.045_1	0.00063
of Middle $I_o(s)$	1.992_7	0.00050	0.045_1	0.00049
of "harmonic" f(r)	1.991_8	0.00021	0.043_6	0.00035
of anharmonic f(r)	$1.992_2 \pm 0.0022$	0.00028	$0.044_2 \pm 0.0032$	0.00045

[a]Total standard deviations

Hexamethylethane

Two separate and completely independent investigations of the hexamethylethane molecule were performed. The sample of hexamethylethane was obtained from the American Petroleum Institute. An NMR investigation indicated that greater than 99 percent of all hydrogens in the sample were equivalent.

Leveled intensities for 21-centimeter, 11-centimeter and 7-centimeter camera distances for Runs I and II are shown in Figures 4 and 5, respectively. The solid backgrounds drawn through the intensity curves are those used in constructing $f_N(r)$; the dashed backgrounds are those obtained by the least squares investigation of the intensity curves. It was discovered too late to make corrections that in photometering of plates in Run I the microphotometer deviated from a linear response when recording absorbancies greater than 0.8. Unfortunately, this caused an excessive curvature in the background for the front portion of the 21-centimeter camera distance curve. The radial distribution curves obtained from $M_N(s)$ curves using a damping factor of $\exp(-.00073s^2)$ are shown in Figures 6 and 7.

If D_3 symmetry is assumed for the carbon skeleton along with threefold symmetry for the methyl groups, the structure of hexamethylethane may be described with seven parameters. The seven parameters chosen were:

(1) r_b average C-C bond length

(2) Δr difference between the central and terminal bond lengths

(3) r_{CH} C-H bond length

(4) α_{CCC} inner CCC bond angle

(5) α_{CCH} CCH bond angle

Figure 4. Hexamethylethane intensity and experimental background curves for long, middle and short camera distances. Run I.

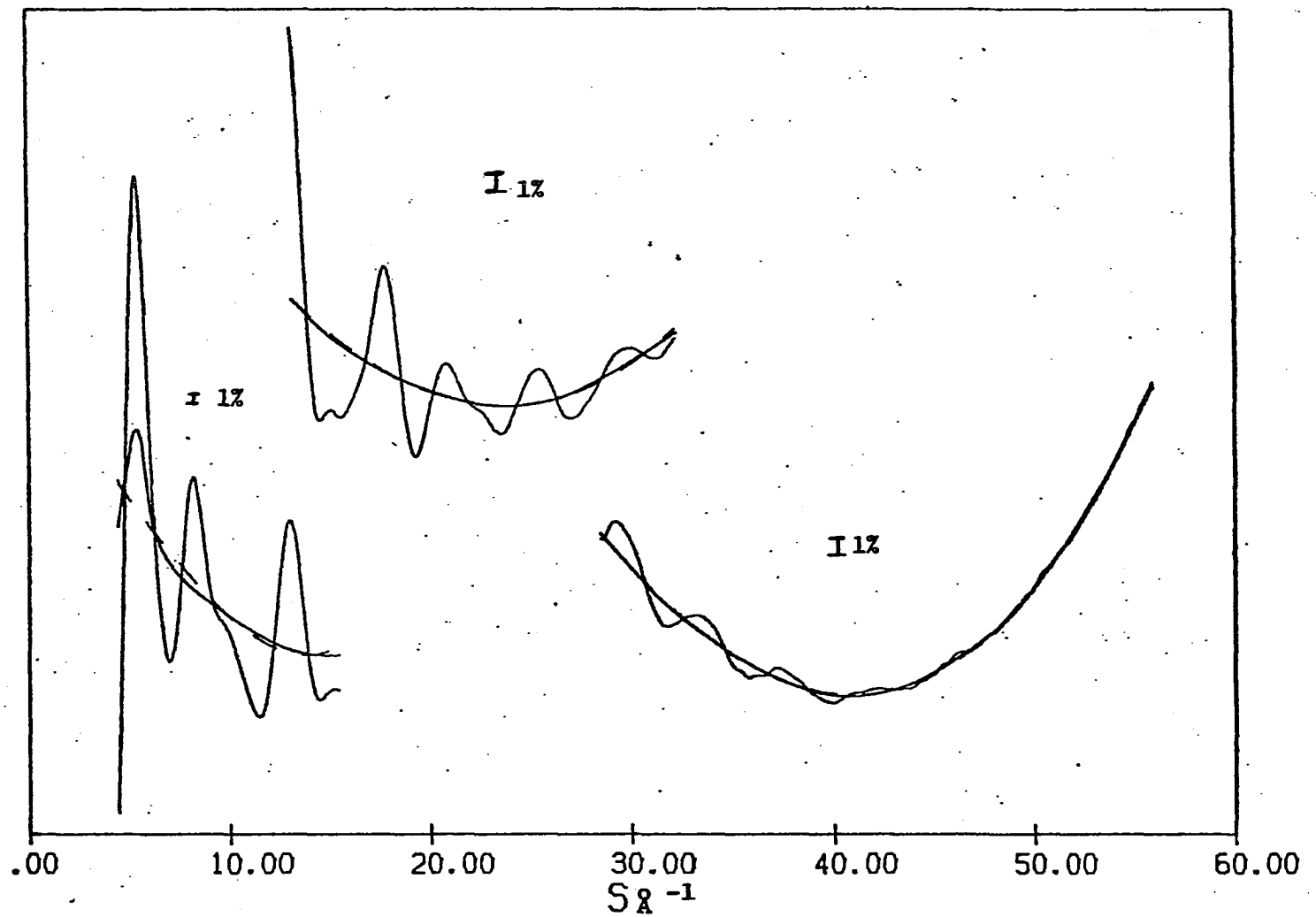
I 1%
I 1%
I 1%
.00
10.00
20.00
30.00
40.00
50.00
60.00
S Å -1

Figure 5. Hexamethylethane intensity and experimental background for long, middle and short camera distances. Run II.

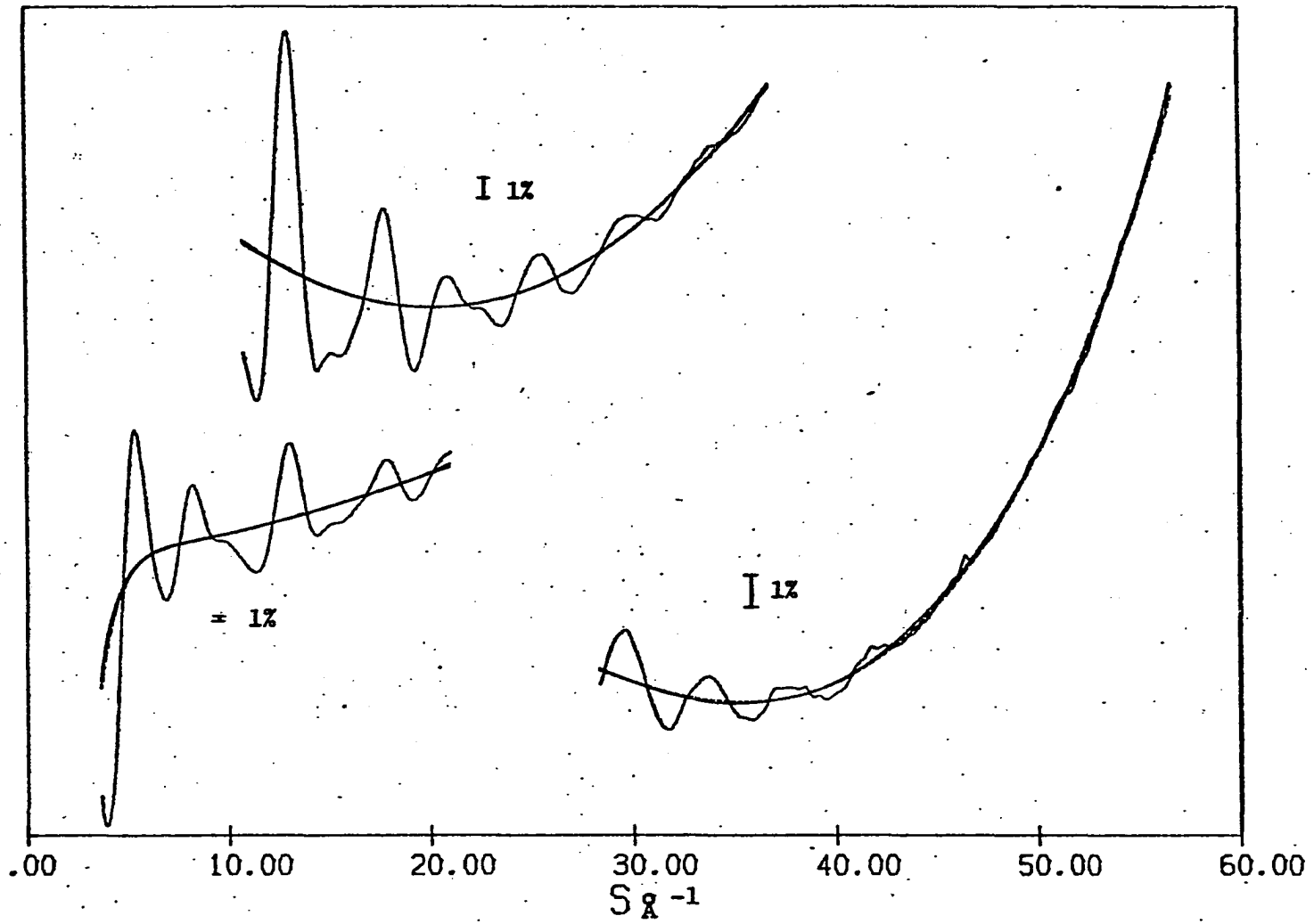
I 1%
± 1%
I 1%
.00
10.00
20.00
30.00
40.00
50.00
60.00
S Å -1

Figure 6. Radial distribution curve of hexamethylethane, Run I. Constructed with

$$N_{CC} = 1.0 - 0.15\exp(-0.0045s^2)$$
$$N_{CH} = 1.0 + 0.14\exp(-0.0020s^2)$$
$$N_{HH} = 1.0 + 0.53\exp(-0.0030s^2).$$

Theoretical curve shown with crosses.

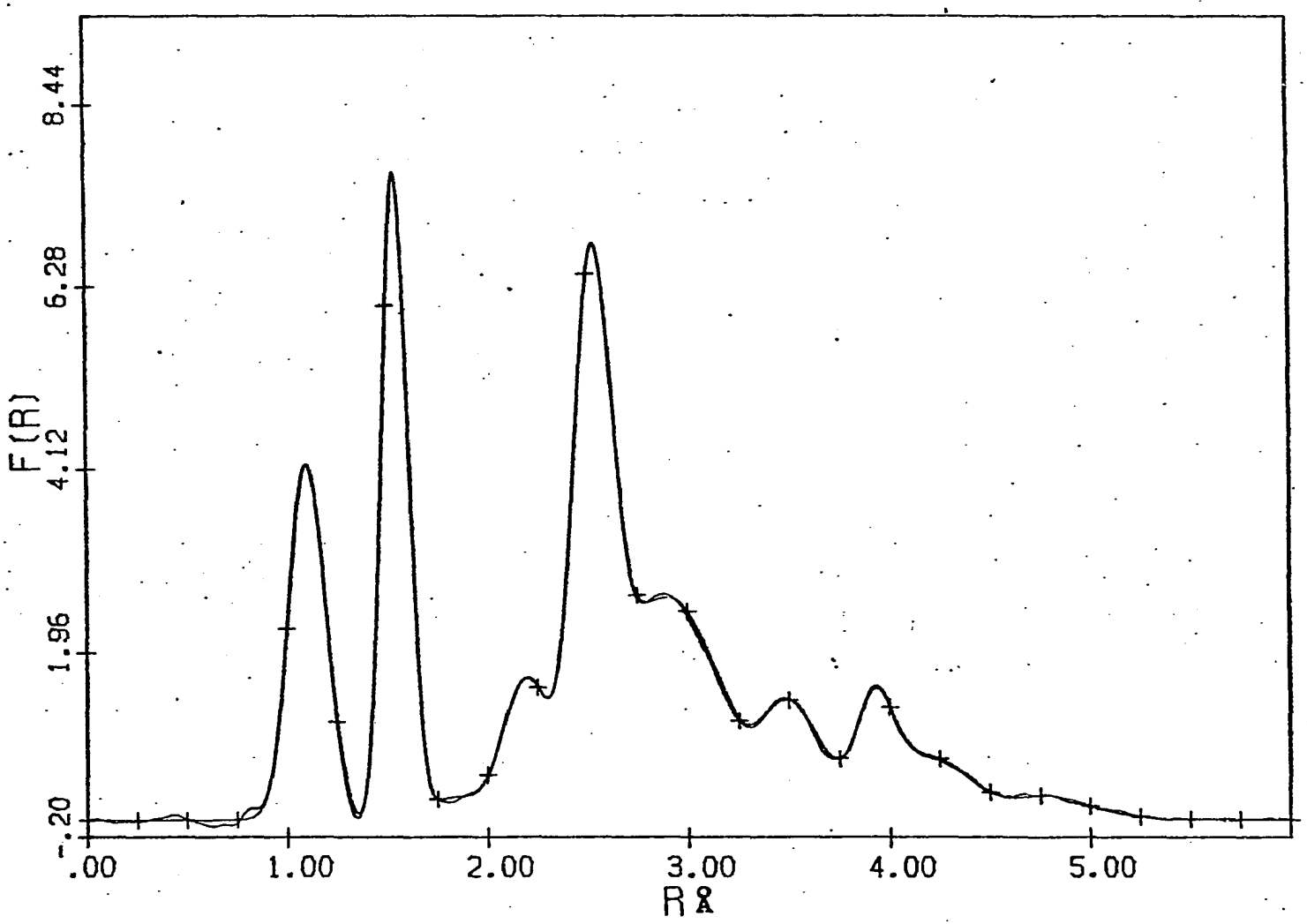
8.44
6.28
4.12
1.96
-.20
F(R)
.00
1.00
2.00
3.00
4.00
5.00
R Å

Figure 7. Radial distribution curve of hexamethylethane. Run II. Constructed with

$$N_{CC} = 1.0 - 0.15\exp(-0.0045s^2)$$
$$N_{CH} = 1.0 + 0.14\exp(-0.0020s^2)$$
$$N_{HH} = 1.0 + 0.53\exp(-0.0030s^2).$$

Theoretical curve shown with crosses.

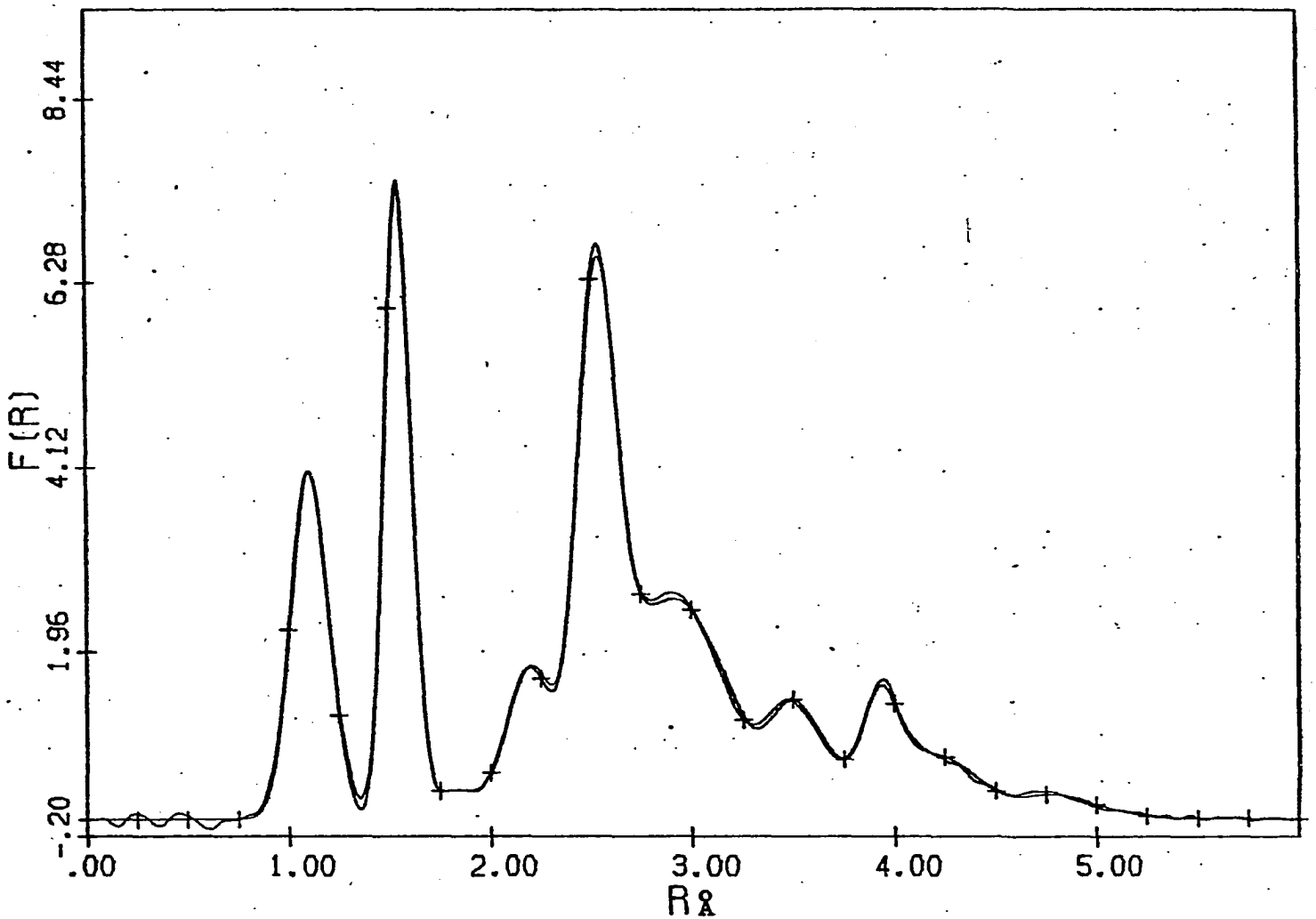
8.44
6.28
4.12
1.96
-.20
F(R)
.00
1.00
2.00
3.00
4.00
5.00
R Å

(6) β_{CC} rotation of one tertiary group with respect to the other (β_{CC} being taken as zero for the eclipsed form (D_{3h}))

(7) β_{CH} rotation of methyl groups about terminal C-C bond (β_{CH} taken as zero when the C-H bonds are eclipsed with the C-C bonds).

The two parameters (β_{CC} and β_{CH}) defining the rotational distortions of the molecule were not varied in the least squares analysis. To determine the value of these parameters a study was made of how the standard deviation between the experimental and theoretical curve changed as a function of changes in these parameters. The two parameters were fixed at certain values and the other five parameters varied in a least squares analysis to obtain an optimum fit of the curve. In Figure 8 is shown a plot of the change in the standard deviation between the curves versus change in one of the parameters. The minima in the curves correspond to β_{CC} = 65 degrees and β_{CH} = 60 degrees. In all least squares investigations reported in this study β_{CC} was fixed at 65 degrees and β_{CH} at 60 degrees.

Since there were only six well resolved peaks in the radial distribution curve, it was felt that only six amplitudes of vibration could be profitably varied in the least squares analysis. For this reason the following limitations were placed on the amplitudes of vibration:

(1) The amplitude of vibration of the central bond was assumed to be 0.001Å greater than the terminal bond amplitudes (difference estimated by extension (44) of Badger's rule (5)).

(2) When two nonbonded C...C distances were less than their amplitude of vibration apart they were constrained to have the same amplitude.

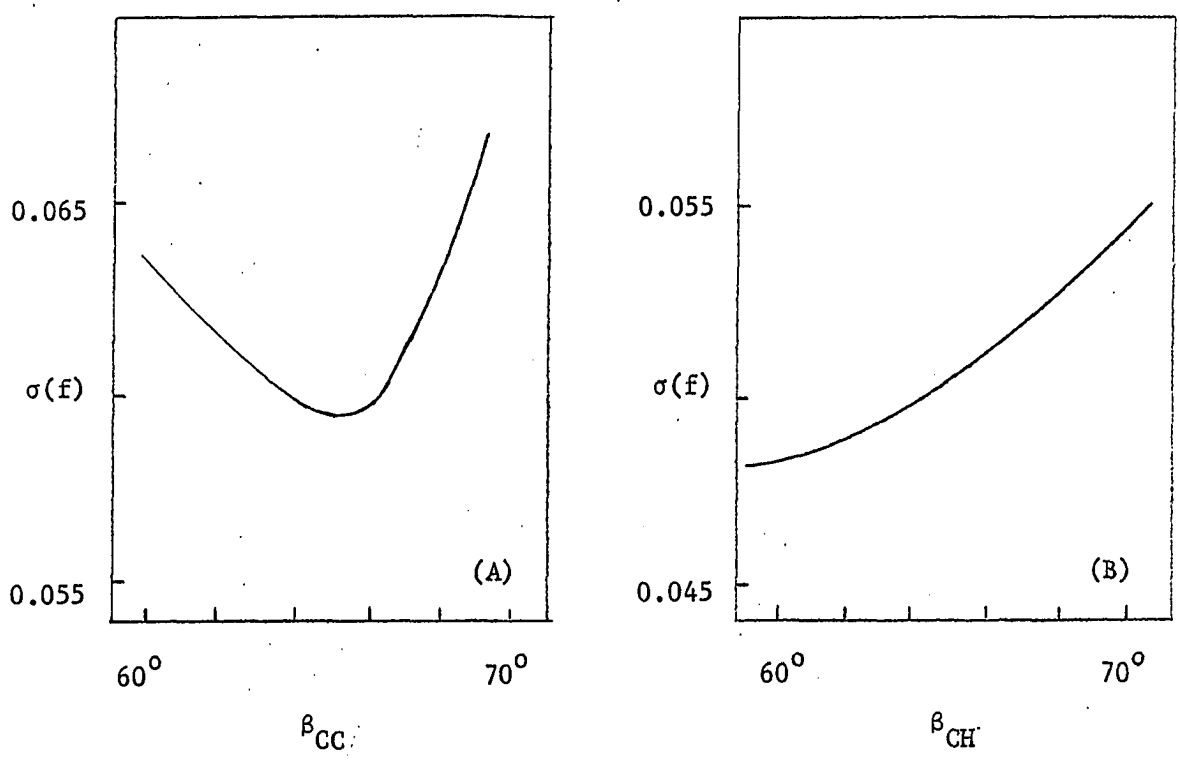

Figure 8. Standard deviation between curves versus change in parameters β_{CC} and β_{CH}. (A) Standard deviation σ(f) versus change in β_{CC}. β_{CH} fixed at 65 degrees. (B) Standard deviation σ(f) versus change in β_{CH}. β_{CC} fixed at 65 degrees.

(3) The amplitudes of all H...H nonbonded distances and all C...H nonbonded distances greater than 2.3Å were fixed at plausible values ranging from 0.13Å to 0.20 Å.

The results of the two runs and the two analyzing techniques are indicated in Tables 3, 4, 5 and 6. In the least squares analysis of the intensity curves, two approaches were applied. The first approach was to allow the background function to vary along with the molecular parameters. In the second approach only the molecular parameters were varied and the background fixed at the values used in constructing the radial distribution curve. The amplitudes of vibration were not varied in the least squares analysis of the intensity curve. They were fixed at the values determined in the analysis of $f_N(r)$ curves. The Bastiansen-Morino shrinkage corrections used in the data analysis are indicated in tables. These values were estimated crudely on the basis of corrections calculated for benzene (47), napthalene (48), dimethylacetylene (49) and a consideration of the shrinkage arising from internal rotations in the molecule (50). Also, the standard deviation $\sigma(r_g)$ of the parameters calculated by the least squares programs (using Equation 14) and an estimated total standard deviation are indicated in the tables.

Tetramethylethane

The sample of tetramethylethane with specified purity greater than 99.8 percent was purchased from Phillips Petroleum Company.

Leveled intensity and background curves for three camera distances are shown in Figure 9. The experimental radial distribution curve for tetramethylethane is shown in Figure 10. The $f_N(r)$ curve was constructed using a damping factor of $\exp(-.00073s^2)$.

Table 3. Results of least squares analysis of radial distribution curve (in Å units) Hexamethylethane. Run I

Independent Parameters			Resulting Internuclear Distances				
Parameter	r_g	$\sigma(r_g)$	Identification	r_g	ℓ_g	$\sigma(\ell_g)$	Shrinkage Correction ($\times 10^4$)
r_b	$1.547_2 \pm 0.002$[a]	0.00020	terminal C-C	1.541_8	$0.053_7 \pm 0.003$[a]	0.0003	00
Δr	0.039 ±0.006	0.0020	central C-C	1.579_8	0.054_7		00
r_{CH}	$1.111_3 \pm 0.003$	0.00057	C....C	2.492_3	$0.074_7 \pm 0.005$	0.0007	05
			C....C	2.572_5	0.074_7		05
α_{CCC}	111.0°_2 ±0.500°	0.038°	C....C	2.994_7	0.14_2 ±0.010	0.0024	20
α_{CCH}	111.7°_4 ±1.00°	0.106°	C....C	3.097_3	0.14_2		20
			C....C	3.931_9	$0.078_8 \pm 0.008$	0.0024	30
β_{CC}	(65°)[b] ±4°		C-H	1.111_2	$0.080_0 \pm 0.004$	0.0004	00
β_{CH}	(60°) ±10°		C....H	2.207_3	$0.110_1 \pm 0.010$	0.0021	20

[a] Estimated total standard deviation

[b] Parameters in parentheses not varied in least squares analysis

Table 4. Results of least squares analysis of radial distribution curve (in Å units). Hexamethylethane. Run II.

Independent Parameters			Resulting Internuclear Distances				
Parameter	r_g	$\sigma(r_g)$	Identification	r_g	ℓ_g	$\sigma(\ell_g)$	Shrinkage Correction ($\times 10^4$)
r_b	$1.547_7 \pm 0.001_8$ [a]	0.00022	terminal C-C	1.542_2	$0.055_1 \pm 0.002_5$	0.0003_5	00
			central C-C	1.580_3	0.056_1		00
Δr	0.041 ±0.006	0.0024	C....C	2.491_1	$0.075_2 \pm 0.005$	0.0006_4	05
			C....C	2.574_9	0.075_2		05
r_{CH}	$1.113_4 \pm 0.002_5$	0.0008_1	C....C	3.000_1	0.138 ±0.01	0.002_6	20
			C....C	3.102_4	0.138		20
α_{CCC}	$111.0_2° \pm 0.50°$	0.038°	C....C	3.935_2	$0.077_2 \pm 0.008$	0.002_7	30
			C-H	1.113_4	$0.082_1 \pm 0.003_5$	0.0005_0	00
α_{CCH}	$111.5_0° \pm 0.80°$	0.135°	C....H	2.206_3	0.105 ±0.01	0.002_0	20
β_{CC}	(65°) [b] ± 4°						
β_{CH}	(60°) ± 10°						

[a] Estimated total standard deviation

[b] Parameters in parentheses not varied in least squares analysis

Table 5. Results of least squares analyses of intensity curves (in Å units). Hexamethylethane. Run I.

Parameter	Background Fixed			Background Varied			Weighted Average[c]
	Long	Middle	Short	Long	Middle	Short	
r_b	$1.548_3\pm$ 0.0009[a]	$1.547_2\pm$ 0.0004	$1.548_3\pm$ 0.001	$1.546_9\pm$ 0.0019	$1.547_3\pm$ 0.0004	$1.548_3\pm$ 0.001	1.547_4
Δr	$0.033_7\pm$ 0.0087	$0.041_1\pm$ 0.0038	$0.043_9\pm$ 0.0066	$0.042_6\pm$ 0.020	$0.041_1\pm$ 0.0042	$0.044_2\pm$ 0.0063	0.041_4
r_{CH}	$1.104_7\pm$ 0.0017	$1.111_7\pm$ 0.0013	(1.111_3)[b]	$1.124_2\pm$ 0.0046	$1.111_5\pm$ 0.0015	(1.111_3)	1.110_4
α_{CCC}	$111.4°_1\pm$ 0.17°	$111.0°_1\pm$ 0.09°	$(111.0°_2)$	$110.8°_5\pm$ 0.36°	$111.0°_2\pm$ 0.10°	$(111.0°_2)$	$111.0°_6$
α_{CCH}	$111.2°_6\pm$ 0.28°	$(111.7°_4)$	$(111.7°_4)$	$111.8°_4\pm$ 0.58°	$(111.7°_4)$	$(111.7°_4)$	$111.3°_7$
R	$1.078\pm$ 0.012	$1.081\pm$ 0.009	$1.082\pm$ 0.04	$1.081\pm$ 0.04	$1.081\pm$ 0.01	$1.083\pm$ 0.04	

[a] Standard deviation of parameter calculated with Equation 14

[b] Parameters in parentheses not varied in least squares analysis

[c] Average calculated by $\bar{z}_k = \sum_{i=1}^{6} [(z_k)_i/\sigma_i^2(z_k)/\Sigma[1.0/\sigma_i^2(z_k)]$

Table 6. Results of least squares analyses of intensity curve (in Å units). Hexamethylethane. Run II.

Parameter	Background Fixed			Background Varied			Weighted Average[c]
	Long	Middle	Short	Long	Middle	Short	
r_b	$1.547_4 \pm$ 0.0008[a]	$1.547_6 \pm$ 0.0003	$1.548_9 \pm$ 0.0013	$1.548_1 \pm$ 0.0011	$1.547_6 \pm$ 0.0003	$1.547_1 \pm$ 0.0015	1.547_6
Δr	$0.049_8 \pm$ 0.0062	$0.039_0 \pm$ 0.0021	$0.043_9 \pm$ 0.0081	$0.036_7 \pm$ 0.011	$0.039_5 \pm$ 0.0020	$0.043_9 \pm$ 0.0098	0.039_9
r_{CH}	$1.112_3 \pm$ 0.0021	$1.113_4 \pm$ 0.0011	(1.113_4)[b]	$1.110_7 \pm$ 0.0024	$1.113_3 \pm$ 0.0010	(1.111_3)	1.113_0
α_{CCC}	$110.9°_2 \pm$ 0.16°	$111.0°_6 \pm$ 0.06°	$(111.1°_3)$	$111.0°_6 \pm$ 0.25°	$111.0°_6 \pm$ 0.08°	$(111.0°_7)$	$111.0°_4$
α_{CCH}	$111.9°_1 \pm$ 0.28°	(111.5°)	(111.5°)	$111.8°_6$ 0.42°	(111.5°)	(111.5°)	111.0_4
R	$0.994 \pm$ 0.0085	$1.0054 \pm$ 0.0052	$1.001 \pm$ 0.04	$0.995 \pm$ 0.015	$1.005 \pm$ 0.005	$1.002 \pm$ 0.05	

[a] Standard deviation calculated with Equation 14

[b] Parameters in parentheses not varied in least squares analysis

[c] Average calculated by $\bar{z}_k = \sum_{i=1}^{6}[(z_k)_i/\sigma_i^2(z_k)]/\Sigma[1.0/\sigma_i^2(z_k)]$

Figure 9. Tetramethylethane intensity and experimental background curves for long, middle and short camera distances

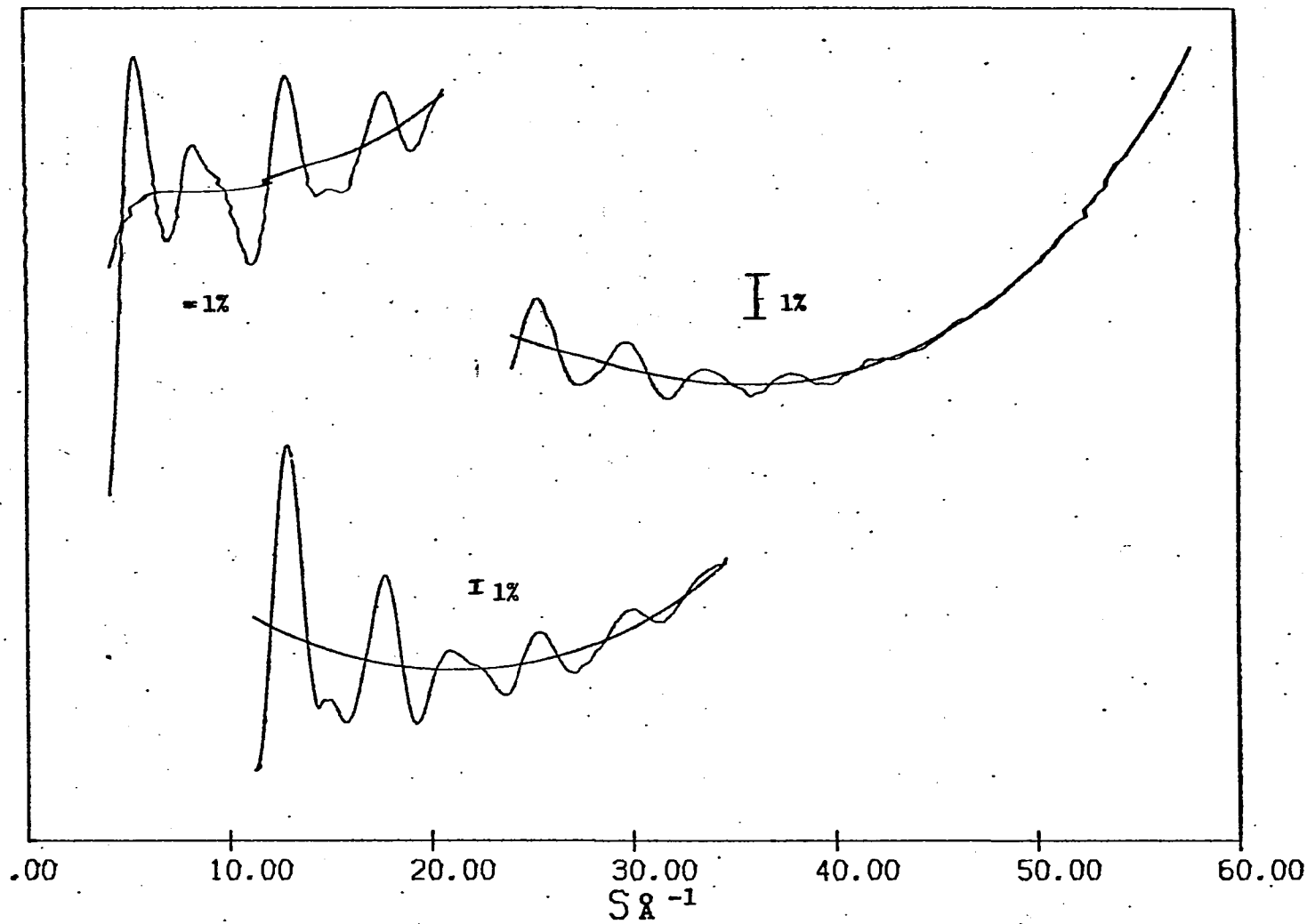
1%
I 1%
I 1%
.00
10.00
20.00
30.00
40.00
50.00
60.00
S Å -1

Figure 10. Radial distribution curve of tetramethylethane. Calculated with

$$N_{CC} = 1.0 - 0.13\exp(-0.0020s^2)$$
$$N_{CH} = 1.0 + 0.14\exp(-0.0020s^2)$$
$$N_{HH} = 1.0 + 0.53\exp(-0.0030s^2).$$

Theoretical curve shown with crosses.

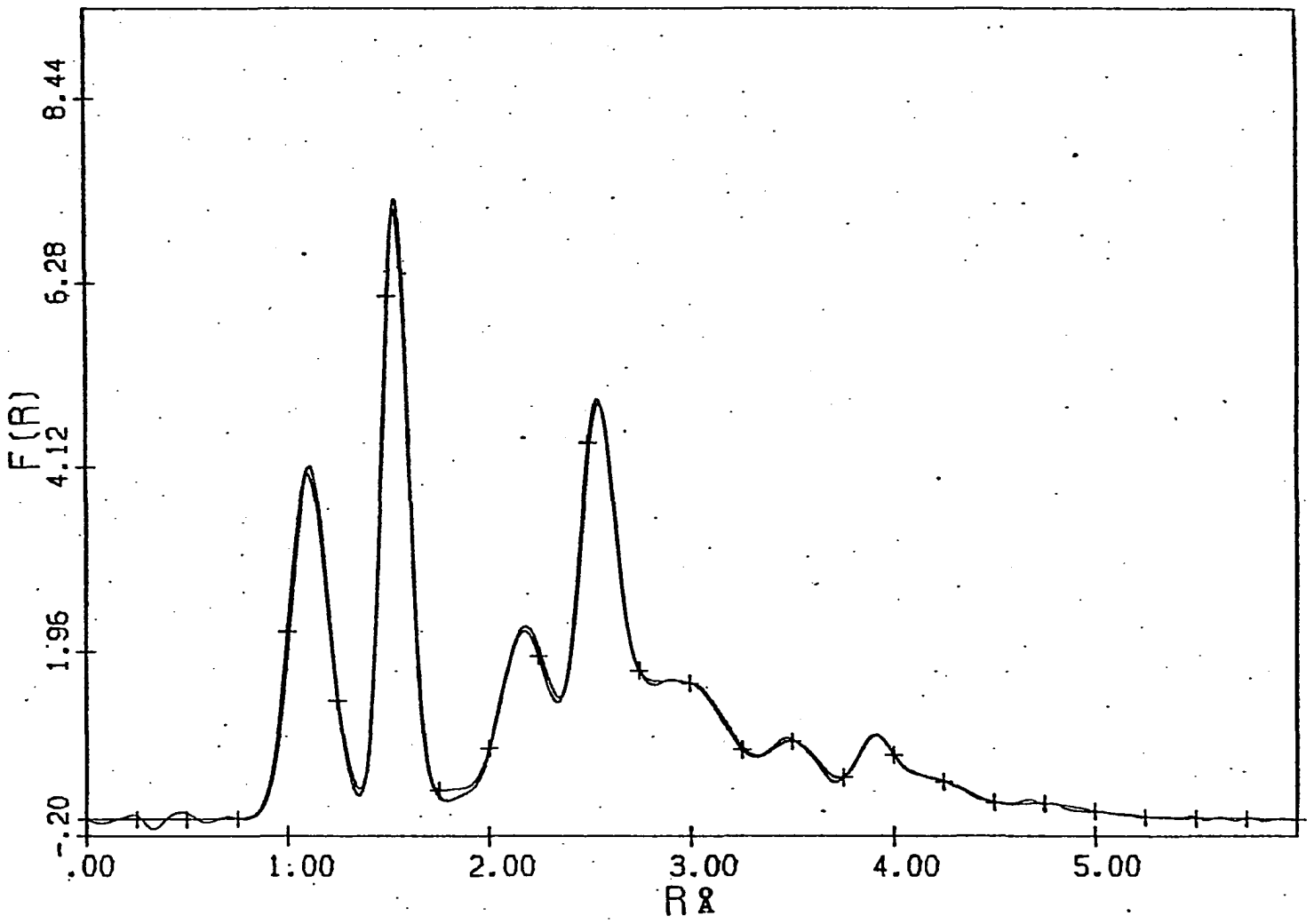
F(R)
8.44
6.28
4.12
1.96
-.20
.00
1:00
2.00
3.00
4.00
5.00
R Å

A gas sample of tetramethylethane at room temperature is a mixture of trans and gauche isomers. Certain assumptions were made in order to reduce the number of parameters that must be determined to define the structure of these two isomers. Both isomers were assumed to have the same terminal C-C bond lengths, identical C-H bond lengths, identical CCH bond angles and identical CCC terminal bond angles. The central C-C bond was assumed to be 0.002Å greater in length in the gauche isomer than in the trans isomer. The basis for this assumption will be discussed in a later section. The trans isomer was assumed to have C_{2h} symmetry, the gauche isomer C_2 symmetry. Two different inner angles were considered in the gauche form. In Figure 11 is a sketch of the carbon skeleton of the gauche isomer. The inner angle $C_1C_2C_3$ was assumed to be different from the $C_1C_2C_4$ angle.

The bonds to the tertiary hydrogens were assumed to be 0.02Å longer than the C-H bonds in the methyl groups. An investigation of the C-H bonded peak in the radial distribution curve indicated that the average C-H bond distance was 1.1146Å. The average C-H bond in hexamethylethane was 1.1134Å. If the C-H bond in the methyl groups of both compounds were identical in length, then the bonds to the tertiary hydrogens must be approximately 0.02Å longer than the methyl C-H bonds, in order to have an average C-H bond length of 1.1146Å in tetramethylethane. The $CCH_{tertiary}$ bond angles were set so that the tertiary hydrogens were an equal distance from each of their three nearest neighbor carbon atoms. On the basis of these assumptions the radial distribution curve was least squared using the following ten parameters:

(1) percent of trans and gauche isomers

(2) r_b average C-C bond length

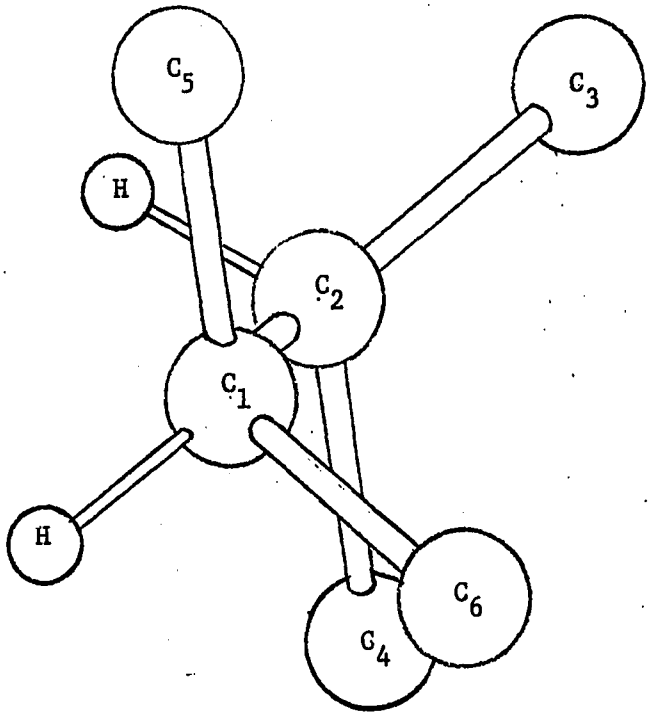

Figure 11. Carbon skeleton of the gauche isomer of tetramethylethane showing the numbering of carbon atoms. The two small balls represent the tertiary hydrogens.

(3) Δr difference in length between central C-C and terminal C-C bonds

(4) r_{CH} C-H bond length in methyl groups

(5) α_{CCC_t} inner CCC bond angle in trans isomer

(6) α_{CCC_g} inner $C_1C_2C_3$ bond angle in the gauche isomer

(7) $\Delta\alpha_{CCC_g}$ angle $C_1C_2C_3$-angle $C_1C_2C_4$

(8) Θ_{CCC} terminal CCC bond angle

(9) α_{CCH} CCH bond angle

(10) β_{CC_g} rotation about the center bond (defined as zero for the eclipsed form C_{2v}).

It was impossible to obtain convergence if all nine of the structural parameters were allowed to vary simultaneously in the least squares process. Therefore, four of the parameters, Δr, Θ_{CCC}, β_{CC_g} and $\Delta\alpha_{CCC_g}$ were fixed at a certain value and the other five parameters varied to obtain the optimum fit. Four new values for the four fixed parameters were then chosen and the process repeated. Plots were made of the deviation between the curves versus each of the four parameter values. Sufficient points were chosen to characterize the minima in the curves. The plots are shown in Figure 12. Each curve has identical values for three of the four parameters, Δr, Θ_{CCC}, β_{CC_g}, and $\Delta\alpha_{CCC_g}$. The parameter specified on the abscissa is the only one varied along a given curve.

It was discovered that the weighted average of all the CCC angles was 111.35 degrees, regardless of the choice of the four fixed parameters. The final models for the two isomers were determined by constraining the weighted average of all the CCC angles to be 111.35 degrees, and using values for

Figure 12. Change in standard deviation between distribution curves versus change in parameters. (A) Standard deviation of curve versus change in Δr. On curve a $\theta_{CCC} = 110^{\circ}$, $\beta_{CC_g} = 66.3^{\circ}$ and $\Delta\alpha_{CCC_g} = 2^{\circ}$. On curve b $\theta_{CCC} = 110^{\circ}$, $\beta_{CC_g} = 66.3^{\circ}$ and $\Delta\alpha_{CCC_g} = 1^{\circ}$. On curve c $\theta_{CCC} = 108^{\circ}$, $\beta_{CC_g} = 66.3^{\circ}$ and $\Delta\alpha_{CCC_g} = 1^{\circ}$. On curve d $\theta_{CCC} = 112^{\circ}$, $\beta_{CC_g} = 66.3^{\circ}$ and $\Delta\alpha_{CCC_g} = 2^{\circ}$. (B) Standard deviation of curve versus change in θ_{CCC_g}. On curve a $\Delta r = 0.005\text{Å}$, $\beta_{CC_g} = 66.3^{\circ}$ and $\Delta\alpha_{CCC_g} = 2^{\circ}$. On curve b $\Delta r = 0.005\text{Å}$, $\beta_{CC_g} = 62.6^{\circ}$ and $\Delta\alpha_{CCC_g} = 0^{\circ}$. (C) Standard deviation of curve versus change in $\Delta\alpha_{CCC_g}$. On curves a,b and c $\Delta r = 0.005\text{Å}$ and $\theta_{CCC} = 110^{\circ}$. On curve a $\beta_{CC_g} = 62.6^{\circ}$, on b $\beta_{CC_g} = 64.6^{\circ}$ and on c $\beta_{CC_g} = 66.3^{\circ}$. (D) Standard deviation of curve versus change in β_{CC_g}. On curves a,b,c and d $\Delta r = 0.005\text{Å}$ and $\theta_{CCC} = 110^{\circ}$. On curve a $\Delta\alpha_{CCC_g} = 0^{\circ}$, on b $\Delta\alpha_{CCC_g} = 1^{\circ}$, on c $\Delta\alpha_{CCC_g} = 2^{\circ}$ and on d $\Delta\alpha_{CCC_g} = 3^{\circ}$.

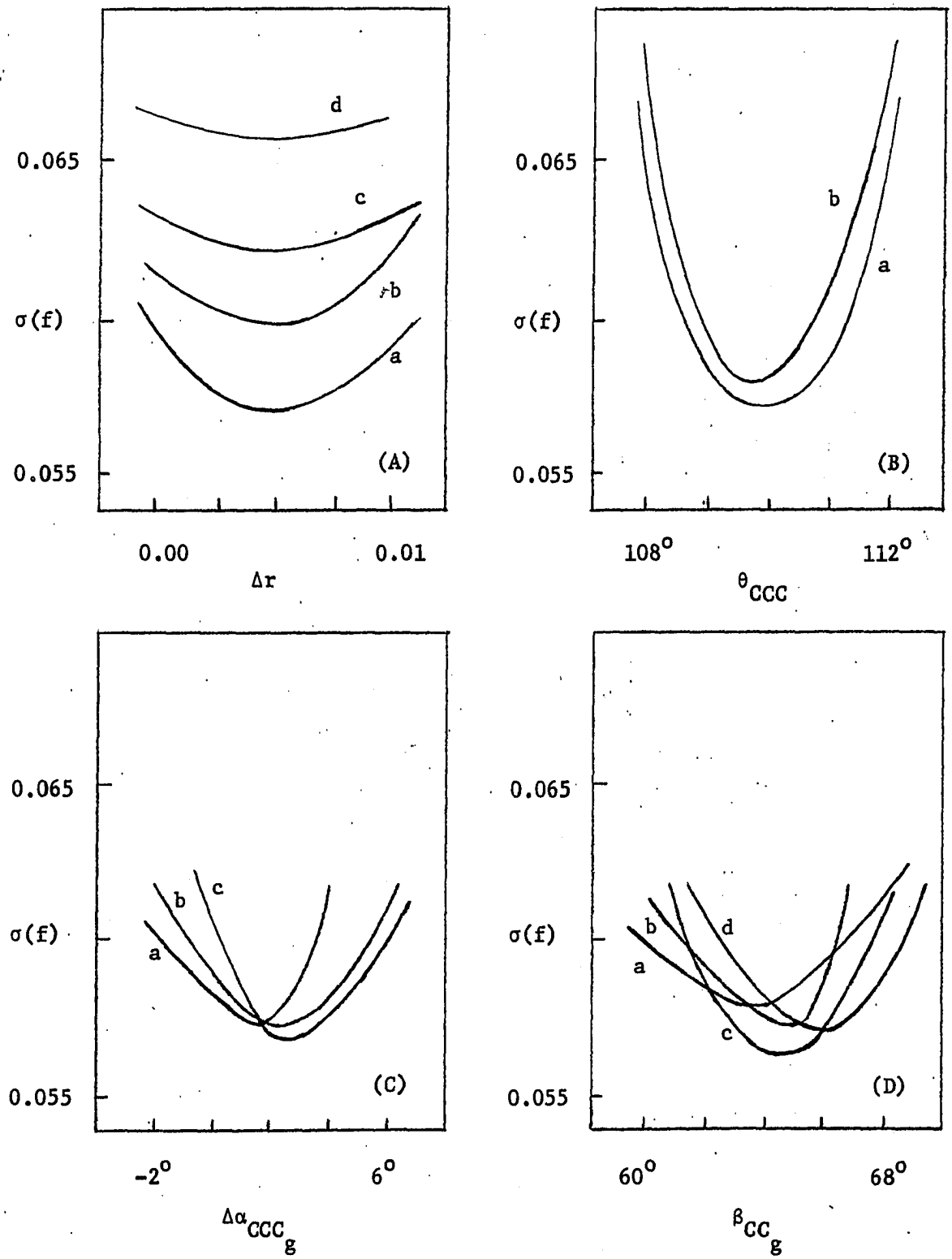
0.065
σ(f)
0.055
d
c
b
a
(A)
0.00
0.01
Δr
0.065
σ(f)
0.055
b
a
(B)
108°
112°
θCCC
0.065
σ(f)
0.055
b
c
a
(C)
-2°
6°
ΔαCCCg
0.065
σ(f)
0.055
b
d
a
c
(D)
60°
68°
βCCg

Δr, θ_{CCC}, β_{CC_g} and $\Delta\alpha_{CCC_g}$ which corresponded to minima in the total deviation curves.

Constraints similar to those used in the hexamethylethane investigation were placed on the amplitudes of vibration in the tetramethylethane analysis. Estimates of shrinkage corrections were made on the same basis as in hexamethylethane.

The results of the least squares investigation are indicated in Table 7. Standard deviations of parameters $\sigma(r_g)$ calculated by the program (using Equation 14) as well as estimates of the total standard deviation are also listed in Table 7.

1,1 Dimethylcyclopropane

Leveled intensities and experimental backgrounds obtained for 1,1 dimethylcyclopropane are shown in Figure 13. The $f_N(r)$ curve obtained from $M_N(s)$ with a damping factor of $\exp(-.00073s^2)$ is shown in Figure 14.

The following assumptions were made in the analysis of 1,1 dimethylcyclopropane:

(1) the three C-C bonds in the cyclopropyl ring were identical in length,

(2) methyl groups had threefold symmetry about the C-C bond,

(3) the C-H bond lengths and HCH angle in the CH_2 groups on the cyclopropyl were equal to 1.100Å and 115 degrees, respectively. These are the values determined by Bastiansen in the investigation of cyclopropane (3).

The structure of 1,1 dimethylcyclopropane may then be described using the following parameters:

Table 7. Results of least squares analysis of radial distribution curve (in Å units). Tetramethylethane.

Independent Parameters			Resulting Internuclear Distances				
Parameter	r_g	$\sigma(r_g)$	Identification	r_g	ℓ_g	$\sigma(\ell_g)$	Shrinkage Correction ($\times 10^4$)
r_b	$1.539_8 \pm 0.002$[a]	0.0002_1	C-H methyl	1.113_6	0.0850 ± 0.006[a]	0.00043	00
			C-H tertiary	1.133_6	0.086_6		00
			C...H methyl	2.190_7	0.110 ± 0.01	0.0014	20
Δr	0.005 ± 0.008		trans isomer[b]				
			terminal C-C	1.537_6	$0.055_4 \pm 0.003$	0.00030	00
			central C-C	1.542_6	$0.055_6 \pm$		00
r_{CH}	$1.113_5 \pm 0.006$	0.0005_5	C...C	2.521_4	$0.075_0 \pm 0.006$	0.00066	05
			C...C	2.540_5	0.075_0		05
α_{CCC_t}	$110.9^\circ_4 \pm 3^\circ$	0.21°	C...C	2.982_2	0.122 ± 0.01	0.0035	20
α_{CCC_g}	$111.0^\circ_6 \pm 3^\circ$	0.13°	C...C	3.904_1	$0.074_6 \pm 0.01$	0.0035	30

[a] Estimated total standard deviation

[b] Results determined with 40 percent trans, 60 percent gauche

Table 7 (continued)

Independent Parameters			Resulting Internuclear Distances				
Parameter	r_g	$\sigma(r_g)$	Identification	r_g	ℓ_g	$\sigma(\ell_g)$	Shrinkage Correction ($\times 10^4$)
			gauche isomer				
$\Delta\alpha_{CCC_g}$	2° - 4° + 3°		terminal C-C	1.537_6	0.055_4		00
			central C-C	1.544_6	0.055_6		00
Θ_{CCC}	$110.0° \pm 2°$		$C_3 \cdots C_4$	2.522_4	0.075_0		05
β_{CC_g}	$65° \pm 5°$		$C_1 \cdots C_3$	2.580_0	0.075_0		05
			$C_1 \cdots C_4$	2.550_1	0.075_0		05
average of CCC angles	$111.3^\circ_5 \pm 0.7°$		$C_3 \cdots C_5$	3.118_3	0.12_2		20
average of inner CCC angles	$112.0^\circ_1 \pm 1.5°$		$C_3 \cdots C_6$	3.119_0	0.12_2		20
			$C_4 \cdots C_5$	3.908_0	0.074_6		30

Figure 13. 1,1 Dimethylcyclopropane intensity and experimental background curves for long, middle and short camera distances

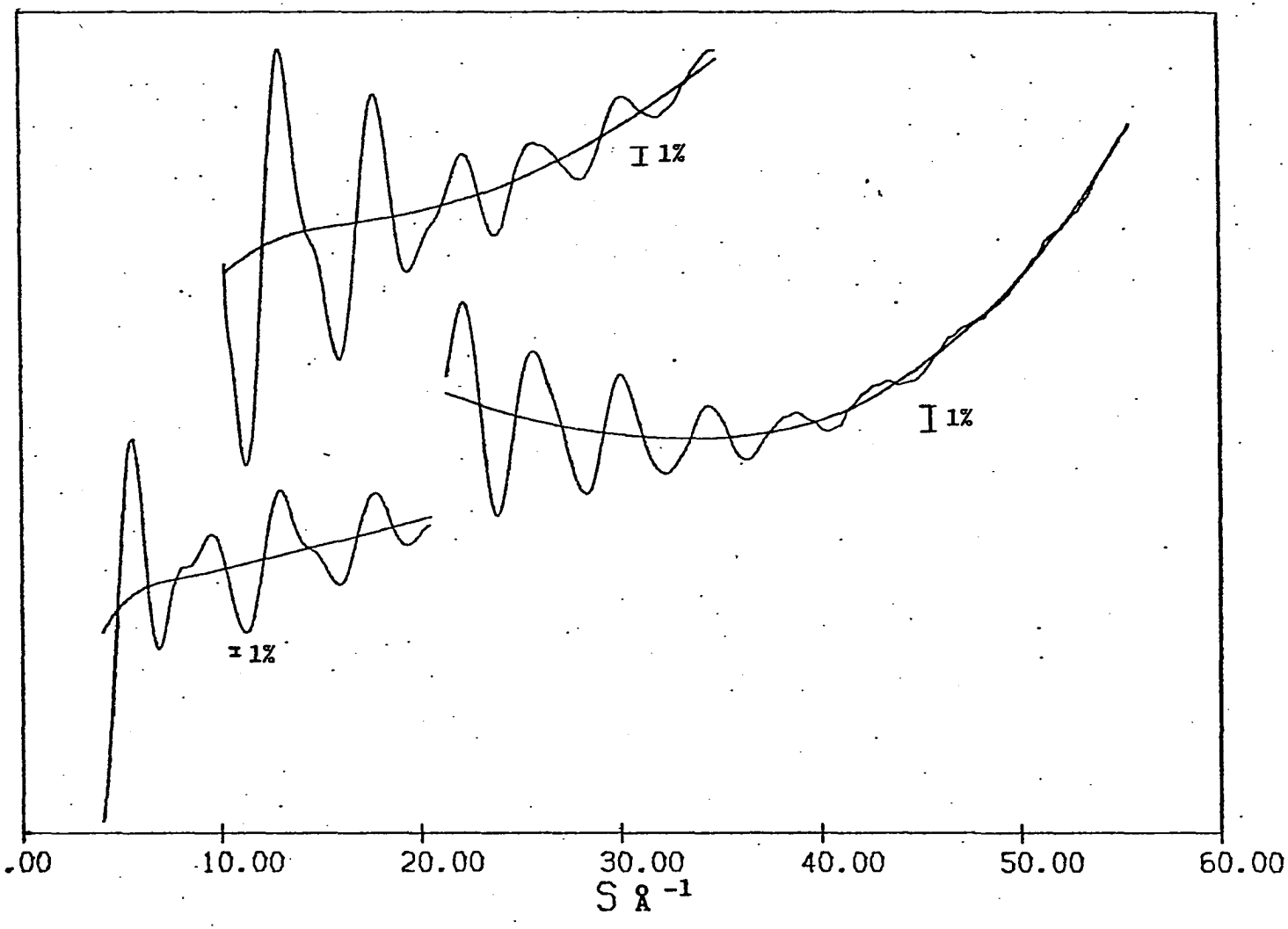
I 1%
I 1%
I 1%
.00
10.00
20.00
30.00
40.00
50.00
60.00
S Å -1

Figure 14. Radial distribution curve for 1,1 dimethylcyclopropane. Constructed with

$$N_{CC} = 1.0 - 0.13\exp(-0.0030s^2)$$
$$N_{CH} = 1.0 + 0.15\exp(-0.0020s^2)$$
$$N_{HH} = 1.0 + 0.45\exp(-0.0020s^2).$$

Theoretical curve shown with crosses.

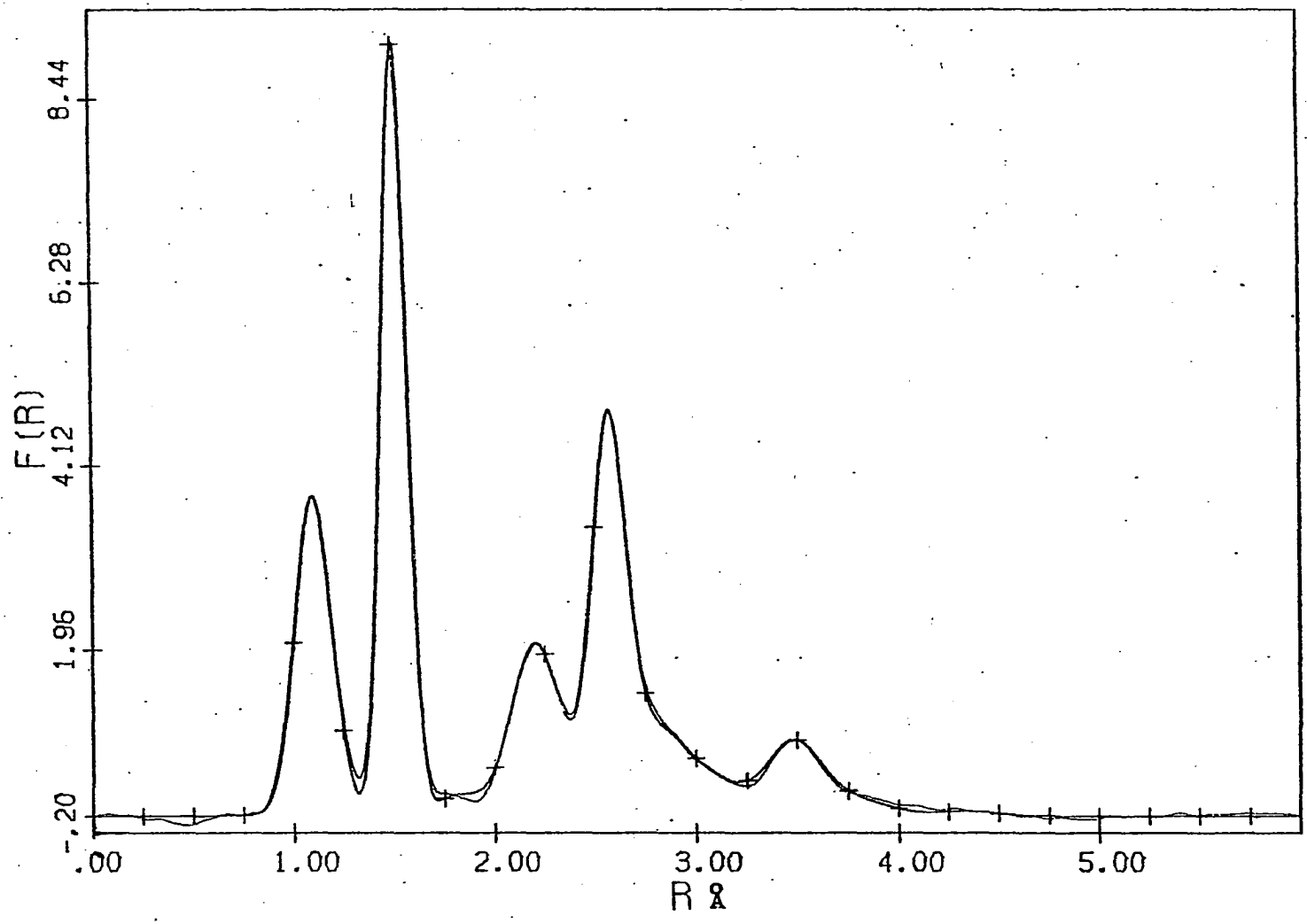
8.44
6.28
4.12
1.96
-.20
F(R)
.00
1.00
2.00
3.00
4.00
5.00
R Å

(1) r_b average C-C bond length

(2) Δr difference in length between the C_r-C_m bonds to methyl groups and the C_r-C_r bonds in the ring (C_r is carbon atom in the cyclopropane ring, C_m is the carbon atom in the methyl group)

(3) r_{CH} C_m-H bond length

(4) α_{CCC} angle $C_mC_rC_m$

(5) α_{CCH} angle C_rC_mH

(6) β_{CH} the orientation of the methyl groups on the C_r-C_m axis (β_{CH} taken as zero when one of the C-H bonds bisects the 60-degree angle in the cyclopropyl ring).

There are only two peaks in the radial distribution curve arising from carbon-carbon distances. Therefore, an approach similar to that used in the analysis of tetramethylethane was employed. The parameter Δr was fixed at certain values and the other four parameters varied to obtain the optimum fit. A plot of the change in total standard deviation of the curve versus the change in Δr is shown in Figure 15. Results of the least squares analysis are reported in Table 8. Amplitudes of vibration, subject to restrictions similar to the hexamethylethane investigation, and the estimated shrinkage corrections are indicated in Table 8.

A study was made of the orientation of the methyl groups on the C_r - C_m axis. The barrier to internal rotation appears to be greater than three kilocalories, with the lowest energy form corresponding to β_{CH} equal to zero.

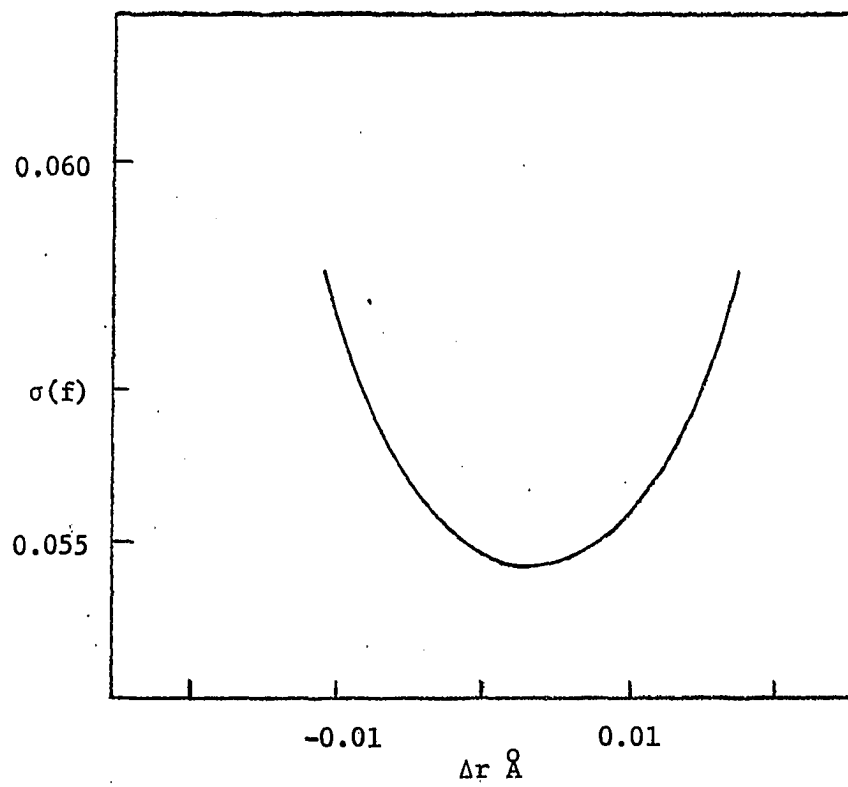

Figure 15. Change in standard deviation between theoretical and experimental radial distribution curves versus difference in C_r-C_m and C_r-C_r bond lengths.

Table 8. Results of least squares analysis of radial distribution curve (in Å units). 1,1 dimethylcyclopropane.

Independent Parameters			Resulting Internuclear Distances				
Parameter	r_g	$\sigma(r_g)$	Identification	r_g	ℓ_g	$\sigma(\ell_g)$	Shrinkage Correction ($\times 10^4$)
r_b	$1.509_2 \pm 0.002$[a]	0.00015	C_r-C_r	1.507_2	$0.053_7 \pm 0.003$[a]	0.0002	00
			C_r-C_m	1.512_2	0.053_7		00
Δr	0.005 ± 0.01		$C_r \ldots C_m$	2.580_6	$0.077_0 \pm 0.008$	0.0005	05
r_{CH}	$1.114_3 \pm 0.008$	0.0005	C_m-H	1.114_3	$0.079_6 \pm 0.006$	0.0004	00
α_{CCC}	$115.7_8° \pm 1.5°$	0.13°	C_r-H	(1.100)[b]	0.079_6		00
α_{CCH}	$110.0_5 \pm 1.5°$	0.23°	$C_r \ldots H$	2.162	$0.10_1 \pm 0.01$	0.0012	02
average C-H	$1.109_8 \pm 0.004$		$C_r \ldots H$	2.243	0.10_1		02

[a] Estimated total standard deviation

[b] Parameter not varied

DISCUSSION OF RESULTS

Chlorine

The four analyzing techniques used in the investigation of chlorine data gave identical results within experimental error. The results agree with those reported by Shibata (9) and by Carroll (10).

On the basis of the agreement of the four separate investigations, it would appear that the least squares programs will give consistent results.

Hexamethylethane

The steric deformations observed in hexamethylethane can be accounted for on the basis of an intramolecular Van der Waals force model (50). Comparison of the C-C bonds in hexamethylethane with the C-C bond of 1.534Å (45,51,52,54) found in normal hydrocarbon chains would indicate a stretching of the central bond of 0.047Å and of the terminal bonds of 0.009Å. The ratio of the lengthening of the central bond to the lengthening of the terminal bond can be explained by simply counting the number of intermethyl forces that act along the bonds. The central bond feels the force of all six interactions with the forces acting parallel to the bond. A given terminal bond would be acted on by two intermethyl forces with the force acting at an angle of 57^{9} to the bond. If the amount of stretching of the bonds is proportional to these forces, then

$$\frac{\text{stretch of central bond}}{\text{stretch of terminal bond}} = \frac{6}{2 \cos 57^{\circ}} = 5.5 .$$

On the basis of this argument one would expect 5.5 times as much stretching of the central bond as of the terminal bond. This ratio is very

close to the observed experimental ratio of 5.2.

The inner angle in hexamethylethane is opened by 1.7° when compared to the tetrahedral angle one would expect in neopentane. The opening of the inner angle is not surprising, but it is interesting to note that the 111° inner CCC angle is actually less than that observed in normal hydrocarbon chains, where the angle is usually 112 to 114 degrees (51,52,53,54). If we consider the 1,3 methyl interactions and note that the terminal bond angles are closed to 108 degrees when the inner angles are opened to 111 degrees, it seems reasonable to expect a smaller inner angle in hexamethylethane than in normal hydrocarbons. The 1,4 methyl interactions force the inner angles to be greater than the terminal angles, but the closing of the 1,3 distance keeps the inner angles from becoming as large as the CCC angles in hydrocarbon chains.

The deformation of the carbon skeleton from D_{3h} symmetry can also be explained on the basis of forces acting between nonbonded atoms. If a model is constructed with D_{3h} symmetry, the hydrogens that are pointing toward the center of the molecule are found to be pointing directly at the hydrogens on the opposite side of the molecule so that H...H nonbonded distance is approximately 2.1Å. A slight rotation about the central bond allows the H...H distances to be increased, thereby lowering the repulsive force and leading to a more stable configuration.

Additional experimental evidence that a distortion is present in the molecule is the large amplitude of vibration observed for the 3.1 gauche distance. This amplitude is greater in hexamethylethane than in tetramethylethane (0.136Å compared to 0.120Å). On the basis of the height of

the barrier to internal rotation, one would expect the 3.1Å gauche distance amplitude of vibration in hexamethylethane to be less than the corresponding amplitude in tetramethylethane. The molecule with a higher rotational barrier would be undergoing less rocking motion about the central bond. The smaller rocking motion would contribute less to the observed amplitude of vibration in hexamethylethane than in tetramethylethane. If the stable configuration, however, corresponded to a five-degree distortion from D_{3d} symmetry, there would then be six energywise degenerate states corresponding to the lowest energy, with minima at +5 and -5 degrees from the staggered configuration. The configuration with β = 55, 60, and 65 degrees would be approximately equivalent in energy with the staggered configuration a slightly higher energy state. This leads to a broadening of the potential well and a greater librating motion, and hence a larger observed amplitude of vibration for the 3.1Å gauche distance.

An additional way of relieving the close H...H nonbonded distances is to shorten the C-H bonds that are pointed towards the center of the molecule and to tilt the methyl groups back off the axis of the terminal C-C bonds. A microwave study of propane (54) has indicated that such distortions of the methyl groups do occur. These distortions were not considered in the present study, but evidence that they may be present in hexamethylethane is that the C-H bonded distance amplitude of vibration is slightly greater than the observed amplitude in normal hydrocarbons (51,52, 53). The larger amplitude of vibration would lead one to believe that there are possibly two different C-H distances under the C-H bonded peak.

It is interesting to speculate on the structure of $(CH_3)_3B\text{-}N(CH_3)_3$ on

the basis of the experimental results obtained for hexamethylethane. Lide (12) interpreted the single rotational constant observed in terms of a long 1.80Å B-N bond. Geller (56), on the other hand, argued that a normal 1.6Å B-N bond was more likely and that the moment of inertia could be explained by an opening of the CBN and CNB angles (perhaps to 113 degrees). If force constants can be used as a measure of the intramolecular forces, one would predict a stretching of the B-N bond of approximately 0.07 - 0.1Å. (The force constant for a B-N bond (57) is approximately half that of a C-C bond (58)). The CNB angle would open about one degree and the CBN angle would open two to four degrees, since H_{CNB} (59) > H_{CCC} (58) > H_{CBN}. One would then predict a B-N bond of 1.71 $\pm$ 0.03Å, a CNB angle of 109.5 - 110.5 degrees, and a CBN angle of 112.0 - 113.5 degrees.

Tetramethylethane

The tetramethylethane data were best fit with a 60 percent gauche-40 percent trans isomer mixture. Spectroscopic investigations have indicated that the energy difference between the rotational isomers of tetramethylethane is very small, with an upper limit of about 100 calories per mole (60,61).

Comparison of the deformations observed in tetramethylethane with those in hexamethylethane indicates that the former has less stretching of the bonds and a greater inner angle opening. The tetramethylethane molecule has the ability to open the dihedral angles to compensate for the opening of the inner angles. Hence, the terminal angles in tetramethylethane are 110 degrees (which is very close to angles observed by Lide for isobutane (62)) and are not closed to the 108 degree terminal angles observed in hexamethylethane. One would predict by comparing the number of 1,4 interactions in

tetramethylethane with the number in hexamethylethane one-third to one-half as much stretch in tetramethylethane as in hexamethylethane. Because of the greater angular opening, however, less than 0.01Å stretch in the central bond is observed. An argument similar to that used in the hexamethylethane discussion can be used to predict the ratio of the central bond stretch to the terminal bond stretch. In the trans isomer there are two 1,4 interacting forces parallel to the central bond and only one acting on each terminal bond, at an angle of 57 degrees.

$$\frac{\text{stretch of central bond}}{\text{stretch of terminal bond}} = \frac{2}{1 \cos 57^\circ} = 2.4.$$

In the gauche isomer there are three 1,4 interacting forces parallel to the central bond while two of the terminal bonds are acted on by two opposing 1,4 forces and the other two terminal bonds are acted on by one force. The double opposing force leads to a greater opening of the $C_1C_2C_3$ angles than the $C_1C_2C_4$ angles.

A greater stretching of the central bond in the gauche isomer than in the trans isomer may be expected. The central bond in the gauche isomer has three 1,4 repulsive interactions acting parallel to the bond while the central bond in the trans isomer has only two. This would lead to one and one-third times as much stretching in the gauche isomer and explains why the stretching of the central bond was taken as 0.002Å greater in the gauche isomer than in the trans.

$$\frac{\text{stretch of central bond in gauche isomer}}{\text{stretch of central bond in trans isomer}} = \frac{3}{2} = 1.5.$$

The greater opening of the $C_1C_2C_3$ and $C_2C_1C_5$ angles in the gauche isomer causes a split in the 3.1Å gauche distances such that the $C_3 \ldots C_6$ distance is greater than the $C_6 \ldots C_4$ distance. This splitting of 3.1Å gauche

distances is offset by an internal rotation of the isomer so that the $C_3 \ldots C_6$ and $C_6 \ldots C_4$ distances remain approximately equal.

1,1 Dimethylcyclopropane

There is a possibility that the bonds in the cyclopropyl ring are not equivalent. This possibility was not investigated in the present study. Microwave studies of halogen derivatives of cyclopropane (14,15) indicated that the bonds in the substituted ring may not be equivalent. The assumption that the C-C bonds in the ring are equivalent, however, should not introduce large uncertainties in the parameters determined in the least squares analysis, since the expected difference in the bond lengths is a few thousandths of an Angstrom unit.

A comparison of the parameters observed in 1,1 dimethylcyclopropane with the parameters in neopentane shows that the $C_m C_r C_m$ angle is opened by approximately six degrees over the tetrahedral angle observed in neopentane, while the C_r-C_m bonds are 0.02Å shorter in length than the 1.534Å C-C bonds found in neopentane. The opening of the angle and the shortening of the bonds may be explained by considering the effective lowering of two 1,3 methyl interactions by formation of the cyclopropane ring. It is interesting to note that the 1,3 C...C distances found in 1,1 dimethylcyclopropane are both longer than the 1,3 C...C distances in neopentane even though the C-C bonds are shorter.

An investigation of the series neopentane, isobutane, propane and 1,1 dimethylcyclopropane shows the change in CCC angles as methyl groups are replaced. In neopentane the 1,3 methyl interactions are balanced and the CCC angles are 109.5 degrees. In isobutane one of the methyls is replaced by a hydrogen and the CCC angles are opened to 111.5 degrees (62). In propane,

two of the methyls are replaced and the CCC angles are opened to 112.4 degrees (54). In 1,1 dimethylcyclopropane the two methyls are tied back so that the 1,3 forces are even further reduced and the CCC angle opened to 115.5 degrees.

An alternative method of explaining the structure of 1,1 dimethylcyclopropane would involve a discussion of the bonding in the cyclopropane ring. The bond angles and bond lengths could be explained on the basis of hybridization of bonds and double bond character. Whether the nonbonded forces are of sufficient magnitude at the appropriate nonbonded distances to explain the structure of 1,1 dimethylcyclopropane without invoking hybridization or double bond character remains to be determined by a more detailed investigation of these forces.

Errors

Uncertainties in structural parameters derived from electron diffraction data may result from either theoretical or experimental deficiencies.

The theoretical expressions employed assume that the energy of incident electrons is extremely large compared to molecular energy levels, that molecular electron densities are the sum of spherical atomic densities, and that effects of polarization and multiple scattering are negligible. Recent calculations of Bonham (64,65,66,67,68) indicate that these assumptions provide reasonable approximations, especially for molecules containing atoms of low atomic numbers.

Experimental errors may be of three different types: (a) measurement of scattering angle and determinations of electron wavelength give rise to systematic errors which affect, primarily, the bond lengths and, secondarily,

the amplitudes; (b) inaccurate emulsion calibration and improper extraneous intensity corrections cause systematic errors affecting the amplitudes of vibration and, possibly, the bond lengths; (c) random errors in the sector calibration curves and random errors due to fluctations in microphotometer readings and emulsion irregularities contribute to uncertainties in both interatomic distances and amplitudes of vibration. These errors do not exhaust all possible sources, but are enough to indicate the primary contributions in these experiments.

The use of Equation 14 to estimate the standard deviation of parameters depends on the assumption that all observed points remain mutually independent. Murata and Morino (68) have demonstrated that correlation among experiment measurables does occur. There are two ways through which correlation is introduced into the observations. It may come in directly from the process of the measurement; it may also be introduced through the process of transformation of the observations, such as Fourier transformation. Murata and Morino have pointed out that correlations which are introduced can be treated by introducing off-diagonal terms into the weight matrix. They propose the use of this off-diagonal weight matrix instead of the diagonal matrix used to obtain Equation 14.

In the present studies the standard deviations $\sigma(z_k)$ reported in tables were obtained from Equation 14 with K the number of observables used to construct the intensity curve. In the analysis of the radial distribution curve, K is taken to be the number of intensity values used in the construction of the distribution curve (not the number of points in the

distribution curve).

Least Squares Analysis

The intensity curve investigation is more direct and less subject to operator bias than the radial distribution analysis. It is also easier to correct for the Born approximation failure in the intensity curve analysis than to evaluate the integrals needed in the $f_N(r)$ analysis. The circle of convergence, however, appears to be more limited in the intensity analysis, and a reasonably good initial guess must be made if meaningful results are to be obtained from the least squares investigations. It appears that the best approach involves the use of both investigating tools with a radial distribution curve constructed at an early stage of the analysis and used as a guide in proposing initial guesses as to the structure of the molecule.

One of the major problems in the analysis of electron diffraction data is determination of the experimental background. One approach is to allow the background to change along with the molecular parameters, as is presently done in the least squares fitting of intensity data. The background, however, also may be determined as the curve that eliminates negative regions in the $f_N(r)$ curve and removes sinusoidal noise patterns that have periods similar or greater in width than the distribution peaks.

One of the best ways of checking for systematic errors is to perform an independent least squares investigation of the data for each camera distance and check how these results compare with one another and with the radial distribution analysis. The parameters obtained from the radial distribution analysis may differ from those obtained from the intensity curve analysis since the points in the intensity curve are not weighted in the same manner in the construction of $M_N(s)$ as in the least squares analysis

of the intensity curve.

Comparison of Two Independent Studies of Hexamethylethane

The two independent investigations of hexamethylethane yield the same results within experimental error, with exception of the investigations of the long camera distance data in Run I. In Figure 16 the intensity curve for the long distance along with a correlation background obtained from

$$I_{B_{corr}} = \frac{I_o(s)}{RM(s)_{theo} + 1}$$

is plotted. At small scattering angles the correlation background contains two humps, one at $s = 6\text{Å}^{-1}$ and the other at $s = 8.5\text{Å}^{-1}$. A curve can be drawn which will follow the sharp curvature in the front portion, but the misfit around $s = 8.5\text{Å}^{-1}$ cannot be fitted unless the criterion of a smooth background is relaxed. This misfit introduces a noise pattern in the $f_N(r)$ curve having a period of 0.8Å. This noise pattern causes a negative region in the probability curve around $r = 1.3\text{Å}$ and affects the center of gravity of both the C-H and C-C bonded peaks. The radial distribution curve shown in Figure 6 was constructed by using theoretical data extending out in space to weight down the influence of nonlinearity of the microphotometer in recording data at small s.

The disagreement between the different analyzing techniques in Run I demonstrates that at least some systematic errors in data can be detected by using different analyzing techniques. The noise patterns in the radial distribution curve reflect that there is an error in the front portion of long camera distance data. The large index of resolution obtained in Run I indicates that the emulsion calibration constants do not accurately

Figure 16. Intensity curve and correlation background for long camera distance data. Run I.

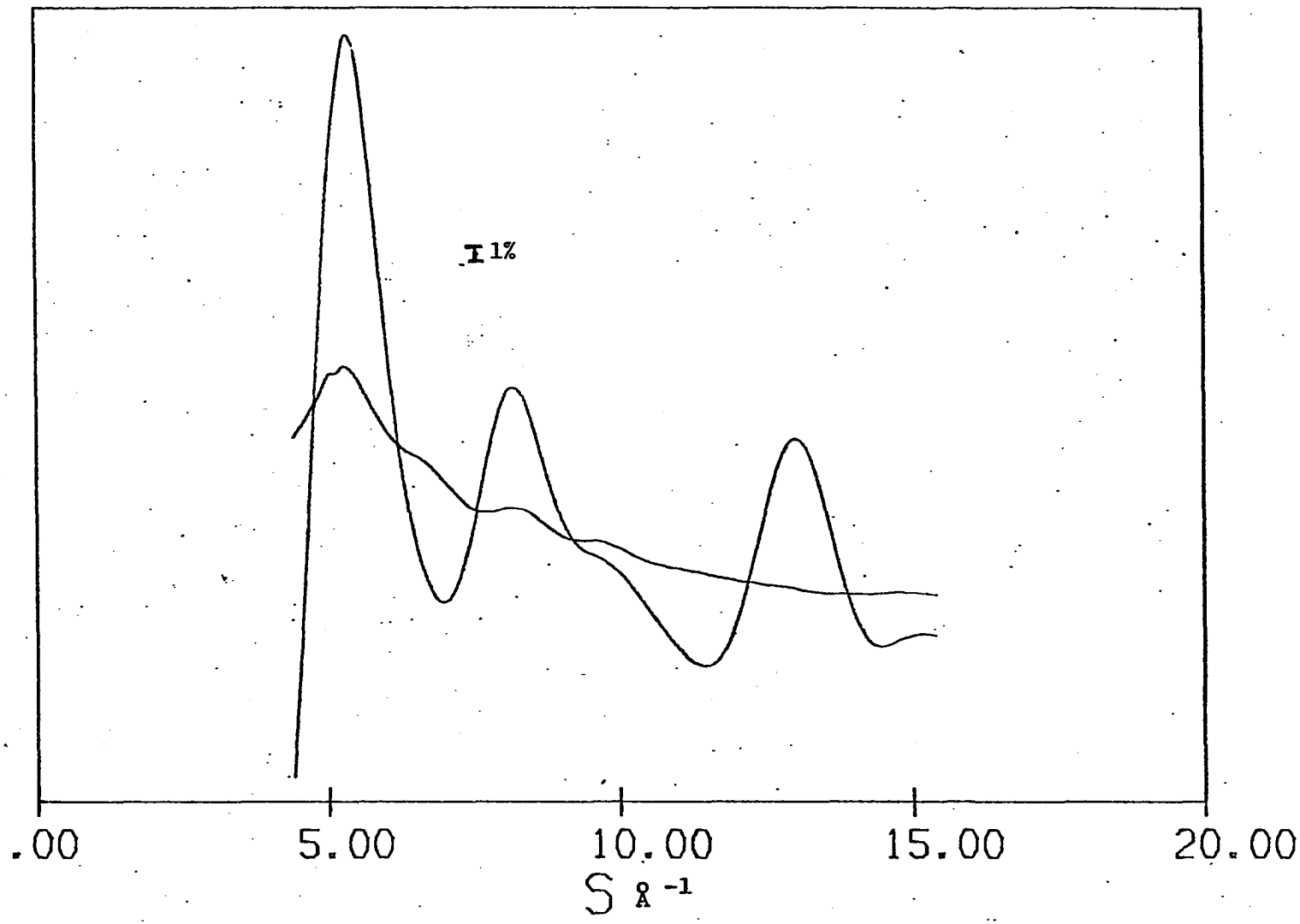
I 1%
.00
5.00
10.00
15.00
20.00
S Å -1

characterize the response of the emulsion surface to the bombarding electrons. The agreement between the amplitudes of vibration obtained in Run I with those determined in Run II, however, demonstrates that much of the error in the emulsion constants can be absorbed in the index of resolution.

SUMMARY

Two least squares programs for analyzing electron diffraction data were developed which imposed geometrical constraints on the internuclear distances. One of the programs was used in the analysis of intensity data and the other in the analysis of radial distribution data. Both programs incorporated more accurate corrections for anharmonicity of vibration and failure of Born approximation than had been used previously. The programs were designed to analyze data directly in terms of a set of geometrically independent internal coordinates. The programs were written to take full advantage of any molecular symmetry properties. A comparison of the two analyzing techniques was made in the determination of several molecular structures.

The molecules selected included hexamethylethane, 1,1,2,2 tetramethylethane and 1,1 dimethylcyclopropane. In each case it was observed that bond lengths and bond angles were deformed when compared to those in simpler reference molecules. In hexamethylethane the central bond was 0.046Å longer than C-C bonds in n-alkanes, and the terminal bonds were stretched by 0.009Å. The inner CCC angles were 111 degrees. The bonds in tetramethylethane were not stretched as much as those in hexamethylethane; nevertheless, the central bond was 0.009Å longer than the normal C-C bond while the terminal bonds were stretched by 0.003Å. The average inner angle in tetramethylethane was 112 degrees. In 1,1 dimethylcyclopropane all the C-C bonds were 0.025Å shorter than the bonds in n-alkanes. The CH_3-C-CH_3 angle of 116 degrees is considerably larger than that found in normal hydrocarbons. A consideration of nonbonded interactions accounted for the observed deformations in bond lengths and bond angles in all three molecules.

LITERATURE CITED

1. Hedberg, K. and Iwasaki, M., Acta Crystallographica 17, 529 (1964).
2. Corbet, H. C., Dallinga, G., Oltmans, F., and Toneman, L. H., Recueil Des Travaux Chimiques Des Pays-Bas T83, 789 (1964).
3. Bastiansen, O., Fritsch, F. N., and Hedberg, K., Acta Crystallographica 17, 538 (1964).
4. Elliot, A., Proceedings of the Royal Society (London) A127, 638 (1930).
5. Badger, R. M., Journal of Chemical Physics 2, 128 (1934).
6. Richards, W. G. and Barrow, R. F., Proceedings of the Chemical Society (London) 1962, 297.
7. Richter, H., Physikalische Zeitschrift 33, 587 (1930).
8. Pauling, L. and Brockway, L. O., Journal of Chemical Physics 2, 867 (1934).
9. Shibata, S., Journal of Physical Chemistry 67, 2256 (1963).
10. Carroll, B. L. Electron Diffraction Investigation of Diborane and Boron-Alkyls. Unpublished Ph.D. thesis. Ames, Iowa, Library, Iowa State University of Science and Technology. 1963.
11. Bauer, S. H. and Beach, J. Y., Journal of the American Chemical Society 64, 1142 (1942).
12. Lide, D. R., Taft, R. W., and Love, P., Journal of Chemical Physics 31 561 (1959).
13. Pauling, L. and Brockway, L. O., Journal of the American Chemical Society 59, 1223 (1937).
14. Schwendeman, R. H., Jacobs, G. D., and Krigas, T. M., Journal of Chemical Physics 40, 1022 (1964).
15. Flygare, W. H., Narath, A., and Gwinn, W. D., Journal of Chemical

Physics 36, 200 (1962).

16. Friend, J. P. and Dailey, B. P., Journal of Chemical Physics 29, 577 (1958).
17. Mott, N. F., Proceedings of the Royal Society (London) A127, 658 (1930).
18. Wierl, R., Annalen der Physik 8, 521 (1931).
19. Debye, P., Journal of Chemical Physics 9, 55 (1941).
20. Bartell, L. S., Journal of Chemical Physics 23, 1219 (1955).
21. Bonham, R. A. and Ukaji, T., Journal of Chemical Physics 36, 72 (1962).
22. Schomaker, V. and Glauber, R., Nature 170, 291 (1952).
23. Ibers, J. A. and Hoerni, J. A., Acta Crystallographica 7, 405 (1954).
24. Bonham, R. A., Journal of Chemical Physics 43, 1460 (1965).
25. Bartell, L. S. and Brockway, L. O., Physical Review 90, 833 (1953).
26. Morse, P. M., Physical Review 34, 57 (1929).
27. Kuchitsu, K. and Bartell, L. S., Journal of Chemical Physics 35, 1945 (1961).
28. Brockway, L. O. and Bartell, L. S., Review of Scientific Instruments 25, 569 (1954).
29. Bartell, L. S., Kuchitsu, K., and DeNeui, R. J., Journal of Chemical Physics 35, 1211 (1961).
30. Hauptman, H. and Karle, J., Physical Review 77, 491 (1950).
31. Atoji, M., Acta Crystallographica 10, 291 (1956).
32. Heisenberg, W., Physikalische Zeitschrift 32, 737 (1931).
33. Bewilogua, L., Physikalische Zeitschrift 32, 740 (1931).
34. Karle, I. J. and Karle, J., Journal of Chemical Physics 17, 1052 (1949).

35. Degard, C., Bulletin de la Societe Royale des Sciences de Liege 6, 383 (1937).

36. Bartell, L. S. and Brockway, L. O., Journal of Chemical Physics 32, 512 (1960).

37. Bonham, R. A. and Bartell, L. S., Journal of Chemical Physics 31, 702 (1959).

38. Viervoll, H., Acta Chemica Scandinavica 1, 120 (1947).

39. Bartell, L. S., Brockway, L. O., and Schwendeman, R. H., Journal of Chemical Physics 23, 1854 (1955).

40. Eyring, H., Physical Review 39, 746 (1932).

41. Bastiansen, O. and Traetteberg, M., Acta Crystallographica 13, 1108 (1960).

42. Morino, Y., Acta Crystallographica 13, 1107 (1960).

43. Morino, Y., Cyvin, S. J., Kuchitsu, K., and Iijima, T., Journal of Chemical Physics 36, 1109 (1962).

44. Bartell, L. S. and Carroll, B. L., Journal of Chemical Physics 42, 1135 (1965).

45. Bartell, L. S., Kohl, D. A., Carroll, B. L., and Gavin, R. M., Journal of Chemical Physics 42, 3079 (1965).

46. Kimura, M. and Iijima, T., Journal of Chemical Physics 43, 2157 (1965).

47. Brooks, W. V. F. and Cyvin, S. J., Spectrochimica Acta 18, 397 (1962).

48. Cyvin, S. J. and Meisingseth, E., Journal of Physical Society Japan 17, Supplement B-II (1962).

49. Almenningin, A., Bastiansen, O., and Munthe-Kaas, T., Acta Chemica Scandinavica 10, 261 (1956).

50. Bartell, L. S., Tetrahedron 17, 1777 (1962).

51. Bartell, L. S. and Kohl, D. A., Journal of Chemical Physics 39, 3097 (1963).

52. Bonham, R. A. and Bartell, L. S., Journal of the American Chemical Society 81, 3491 (1961).

53. Bartell, L. S. and Higginbotham, H. K., Journal of Chemical Physics 42, 851 (1965).

54. Lide, D. R., Journal of Chemical Physics 33, 1514 (1960).

55. Morrison, J. D. and Robertson, J. M., Journal of Chemical Society (London) 17, 1001 (1949).

56. Geller, S., Journal of Chemical Physics 32, 1569 (1960).

57. Taylor, R. C., Advances in Chemistry Series 1966, 59.

58. Schachtschneider, J. H. and Snyder, R. G., Spectrochimica Acta 19, 117 (1963).

59. Rice, B., Galiano, R. J., and Lehman, W. J., Journal of Physical Chemistry 61, 1222 (1957).

60. Scott, P. W., McCullough, J. P., Williamson, K. D., and Waddington, G., Journal of the American Chemical Society 73, 1707 (1951).

61. Brown, J. K. and Sheppard, N., Journal of Chemical Physics 19, 976 (1951).

62. Lide, D. R. and Mann, D. E., Journal of Chemical Physics 29, 914 (1958).

63. Iijima, T., Bonham, R. A., and Ando, T., Journal of Physical Chemistry 67, 1472 (1963).

64. Bonham, R. A. and Iijima, T., Journal of Physical Chemistry 67, 2266 (1963).

65. Bonham, R. A., Journal of Chemical Physics 43, 1460 (1965).

66. Bonham, R. A., Journal of Chemical Physics 43, 1460 (1965).

67. Bonham, R. A., Journal of Chemical Physics 43, 1933 (1965).

68. Bonham, R. A., Journal of Chemical Physics 43, 1103 (1965).

69. Murata, Y. and Morino, Y., Acta Crystallographica 20, 605 (1966).

APPENDIX

The theoretical expression used in the least squares analysis of $f_N(r)$ when corrections are made for failure of Born approximation (21,22,23) is

$$f_N(r)_{calc} = \sum_i \sum_{j\neq i} \{\delta_+(r) + \delta_-(r) + i_{2+} + i_{2-} + i_{3+} + i_{3-}$$

$$+ A_{ij}(c_{ij}/2(r_e)_{ij})[a_{ij}(\frac{\alpha_{ij}\pi}{\gamma_{ij}})^{1/2} E_{3-5}(x)_{ij} \exp(-\alpha_{ij}x_{ij}^2/\gamma_{ij})$$

$$+ b_{ij}(\frac{\alpha_{ij}\pi}{\gamma'_{ij}})^{1/2} E'_{3-5}(x)_{ij} \exp(-\alpha_{ij}x'^2_{ij}/\gamma_{ij})]\}$$

where

$$E_{3-5}(x)_{ij} = \sum_{n=3}^{5} (\varepsilon'_n)_{ij}\gamma^{-n})_{ij} x_{ij}^n$$

$$E'_{3-5}(x)_{ij} = \sum_{n=3}^{5} (\varepsilon'_n)_{ij}\gamma'^{-n}_{ij} x_{ij}^n$$

$$\delta_{\pm}(r) = a_{ij} f_{\pm}(r) + b_{ij} f'_{\pm}(r)$$

$$i_{2_{\pm}} = a_{ij} I_{2_{\pm}} + b_{ij} I'_{2_{\pm}}$$

$$i_{3_{\pm}} = a_{ij} I_{3_{\pm}} + b_{ij} I'_{3_{\pm}}$$

$$f_{\pm}(r) = [c_{ij}/4(r_c)_{ij}](\pi/2)^{1/2}[(\ell_c^2)_{ij} + 2b]^{-1/4}(\sigma_1)^{-1/4}$$

$$X \exp(-(x_{\pm}^2)_{ij}/2\sigma_1) \cos[A' + (x_{\pm}^2)_{ij}/2\sigma_2]$$

$$I_{2_{\pm}} = \pm(x_{\pm})_{ij}/\sigma_1 \int_0^1 d\theta \{\exp[-(x_{\pm})_{ij}^2/2\sigma_1(1-(\ell_c^2)_{ij}\theta^2/\sigma_1)]$$

$$\cos[-\Delta c_{ij}(x_{\pm})_{ij}^2\theta^2/\sigma_1^2 - (x_{\pm}^2)_{ij}/(2\sigma_2) + \pi/2]\}$$

$$I_{3_{\pm}} = \mp(x_{\pm})_{ij}/\sigma_2 \int_0^1 d\theta \{\exp[(-\ell_c^2)_{ij}(x_{\pm}^2)_{ij}\theta^2/(2\sigma_2^2)$$

$$+ 2\Delta c_{ij}(x_{\pm}^2)_{ij}\theta/\sigma_1\sigma_2 - (x_{\pm}^2)_{ij}/2\sigma_1$$

$$+ (\ell_c^2)_{ij}(x_{\pm}^2)_{ij}/2\sigma_1^2] \cos[(\Delta c_{ij}(x_{\pm}^2)_{ij}/\sigma_2^2)\theta^2$$

$$+ (\ell_c^2)_{ij}(x_{\pm}^2)_{ij}\theta/\sigma_1\sigma_2 - (x_{\pm}^2)_{ij}/2\sigma_2 - \Delta c_{ij}(x_{\pm}^2)_{ij}/\sigma_1^2 + \Delta a_{ij}]\}$$

$$(x_{\pm})_{ij} = r - (r_c)_{ij} \pm \Delta b_{ij}$$

$$\sigma_1 = (\ell_c^2)_{ij} + 2b + 4\Delta c_{ij}^2/[(\ell_c^2)_{ij} + 2b]$$

$$\sigma_2 = 2\Delta c_{ij} + [(\ell_c^2)_{ij} + 2b]^2/2\Delta c_{ij}$$

$$A' = 0.5 \arctan [2\Delta c_{ij}/((\ell_c^2)_{ij} + 2b)] + \Delta a_{ij}[4\Delta c_{ij}^2 + ((\ell_c^2)_{ij} + 2b)^2]/[(\ell_c^2)_{ij} + 2b]\sigma_1$$

where $(r_c)_{ij}$ and $(\ell_c)_{ij}$ are related to $(r_e)_{ij}$ and $(\ell_\alpha)_{ij}$ by Equations 25 and 26 in Reference 27. The terms $I'_{2_\pm}$ and $I'_{3_\pm}$ are similar to $I_{2_\pm}$ and $I_{3_\pm}$, respectively. The difference is that in the primed integrals the damping factor b is replaced by $b + \beta_{ij}$. The additional terms are defined by the equations

$$N_{ij} = a_{ij} + b_{ij} \exp(-\beta_{ij}s^2)$$

$$\cos(\Delta\eta_{ij}) = \cos(\Delta a_{ij} + \Delta b_{ij}s + \Delta c_{ij}s^2)$$

$$\Delta a_{ij} = a_i - a_j$$

$$\Delta b_{ij} = b_i - b_j$$

$$\Delta c_{ij} = c_i - c_j$$

and

$$a_i = 0.1904 \exp(0.0042222Z_i) - 0.168 \exp(-0.06980Z_i)$$

$$b_i = 0.1091 \exp(0.005066Z_i) - 0.1084 \exp(-0.02784Z_i)$$

$$c_i = -0.0007592 \exp(0.006103Z_i) + 0.0007543 \exp(-0.04212Z_i)$$

A synthetic radial distribution curve was constructed from a theoretical

$M_N(s)$ curve calculated for a hypothetical model of XeF_2 with an Xe-F distance of r_g = 2.0013Å, ℓ_α = 0.050Å and an a_{ij} value of 2.5Å^{-1}. A plot of this curve is shown in Figure 17. Along with this $f_N(r)$ plot are three curves showing the difference between theoretical $f_N(r)$ curves. Difference curve A is

$$[f_N(r)_{M_N} - f_N(r)_{LS}]$$

where $f_N(r)_{M_N}$ is the curve obtained from the inversion of the theoretical $M_N(s)$ curve and $f_N(r)_{LS}$ is the curve obtained by using expressions in the least squares program. Difference curve B is

$$[f_N(r)_{M_N} - f'_N(r)_{LS}]$$

where $f'_N(r)_{LS}$ is obtained from the expressions in the least squares program without including the additional Born approximation corrections I_2 and I_3 due to Kimura and Iijima (46). Difference curve C shows the difference between $f_N(r)_{M_N}$ and a curve calculated with Equation 18 without any Born approximation corrections being included.

A least squares analysis of the $f_N(r)_{M_N}$ curve was performed starting with an initial model with r_g for Xe-F = 1.9913Å, ℓ_α = 0.053Å and a = 2.5Å^{-1}. The converged set of parameters obtained were r_g = 2.0014 and ℓ_α = 0.0501Å.

Figure 17. Comparison of theoretical radial distribution curves calculated for a hypothetical model of XeF_2. (A) Difference curve A. (B) Difference curve B. (C) Difference curve C.

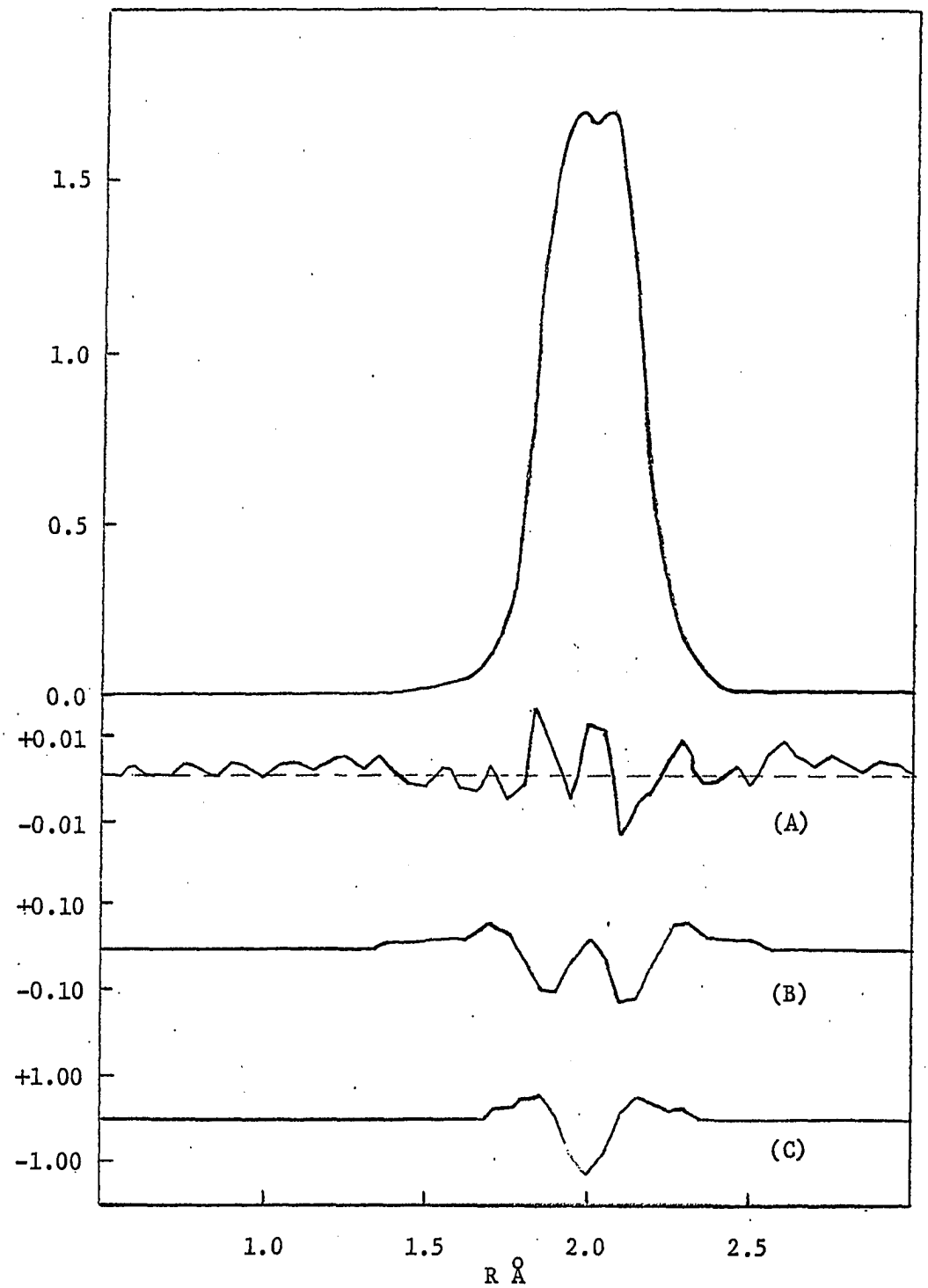
1.5
1.0
0.5
0.0
+0.01
-0.01
(A)
+0.10
-0.10
(B)
+1.00
-1.00
(C)
1.0
1.5
2.0
2.5
R Å

ACKNOWLEDGEMENTS

I would like to thank Dr. L. S. Bartell for suggesting the problems discussed in this dissertation and for his guidance throughout my studies.

My thanks to Dr. R. M. Gavin for his willingness to discuss research problems and for his helpful advice. I also want to thank Mr. F. B. Clippard for his help in the analysis of hexamethylethane data.

I would like to thank Dr. E. A. Roth for taking the diffraction pictures of 1,1 dimethylcyclopropane.

For their aid and advice, I wish to express my gratitude to Dr. H. B. Thompson, Mr. G. J. Janzen and Miss E. J. Jacob.

I am indebted to National Science Foundation for financial support throughout this research.

Special thanks to the members of my family for their encouragement during the course of this study.